Effects of alternative electron acceptors on the activity and community structure of methane-producing and -consuming microbes in the sediments of two shallow boreal lakes

Antti J. Rissanen[1,3,*], Anu Karvinen[2], Hannu Nykänen[3,4], Sari Peura[3,5], Marja Tiirola[3], Anita Mäki[3], Paula Kankaala[2]

1) Tampere University of Technology, Laboratory of Chemistry and Bioengineering, Tampere, Finland

2) University of Eastern Finland, Department of Environmental and Biological Sciences, Joensuu, Finland

3) University of Jyväskylä, Department of Biological and Environmental Science, Jyväskylä, Finland

4) University of Eastern Finland, Department of Environmental and Biological Sciences, Kuopio, Finland

5) Swedish University of Agricultural Sciences, Science for Life Laboratories, Department of Forest Mycology and Plant Pathology, Uppsala, Sweden

***Corresponding author**: Tampere University of Technology, Laboratory of Chemistry and Bioengineering, P.O. Box 541, FI-33101, Tampere, Finland

E-mail: antti.rissanen@tut.fi, Tel: +358 40 1981145, Fax: +358 3 3641392

One sentence summary: Anaerobic methane oxidation did not have any ecological relevance in the methane consumption in the sediments of two shallow boreal lakes.

ABSTRACT

The role of anaerobic CH_4 oxidation in controlling lake sediment CH_4 emissions remains unclear. Therefore, we tested how relevant EAs (SO_4^{2-}, NO_3^-, Fe^{3+}, Mn^{4+}, O_2) affect CH_4 production and oxidation in the sediments of two shallow boreal lakes. The changes induced to microbial communities by the addition of Fe^{3+} and Mn^{4+} were studied using next-generation sequencing targeting the 16S rRNA and methyl-coenzyme M reductase (*mcrA*) genes and *mcrA* transcripts. Putative anaerobic CH_4 oxidizing archaea (ANME-2D) and bacteria (*NC 10*) were scarce (up to 3.4% and 0.5% of archaeal and bacterial 16S rRNA genes, respectively), likely due to the low environmental stability associated with shallow depths. Consequently, the potential anaerobic CH_4 oxidation (0–2.1 nmol $g^{-1}_{\text{dry weight (DW)}}d^{-1}$) was not enhanced by the addition of EAs, nor important in consuming the produced CH_4 (0.6–82.5 nmol $g^{-1}_{DW}d^{-1}$). Instead, the increased EA availability suppressed CH_4 production via the outcompetition of methanogens by anaerobically respiring bacteria and via the increased protection of organic matter from microbial degradation induced by Fe^{3+} and Mn^{4+}. Future studies could particularly assess whether anaerobic CH_4 oxidation has any ecological relevance in reducing CH_4 emissions from the numerous CH_4-emitting shallow lakes in boreal and tundra landscapes.

Keywords: lake, sediment, methanogenesis, methane oxidation, 16S rRNA, *mcrA*

INTRODUCTION

Lake sediments are globally important carbon stores (Molot and Dillon 1996; Kortelainen *et al*. 2004), but they are also important contributors of methane (CH_4) to the atmosphere (Bastviken *et al*. 2004). CH_4 emissions from these environments are controlled by both methanogenesis and CH_4 oxidation. Methanogenesis is the final step in organic matter (OM) degradation, during which methanogenic archaea produce CH_4 from either acetate via the acetoclastic pathway or by oxidizing H_2 using CO_2 as an electron acceptor (EA) via the hydrogenotrophic pathway (Conrad 1999). Some archaea can also produce CH_4 from other methyl compounds (e.g. methanol) via the methylotrophic pathway (Conrad 1999; Borrel *et al*. 2013). The substrates necessary for methanogenesis are produced by fermentative and syntrophic bacteria (Conrad 1999). In oxic conditions, CH_4 is efficiently consumed through aerobic oxidation (MO) by methanotrophic bacteria (MOB) utilizing O_2 as an EA (e.g. Hanson and Hanson 1996). In anoxic conditions, CH_4 consumption can potentially proceed through anaerobic oxidation (AOM) by anaerobic methanotrophic archaea (ANME archaea) utilizing various inorganic (Beal, House and Orphan 2009; Knittel and Boetius 2009; Haroon *et al*. 2013; Ettwig *et al*. 2016) and organic (Scheller *et al*. 2016) compounds or bacteria of the *NC 10* phylum utilizing NO_2^- (Ettwig *et al*. 2010) as EAs. While AOM coupled with SO_4^{2-} - reduction dominates anaerobic CH_4 oxidation in marine sediments (Knittel and Boetius 2009), the limited existing evidence suggests that AOM, coupled with the reduction of various inorganic EAs, i.e. SO_4^{2-} (Timmers *et al*. 2016), NO_3^-/NO_2^- (Deutzmann *et al*. 2014; á Norði and Thamdrup 2014), Fe^{3+} (Sivan *et al*. 2011) and Mn^{4+} (Segarra *et al*. 2013), could be important in freshwater systems. Furthermore, some methanogens oxidize small amounts of CH_4 without external EAs

during trace methane oxidation (TMO) due to enzymatic backflux (Moran *et al*. 2005; Timmers *et al*. 2017).

In temperate and boreal lakes, the sediment EA availability varies seasonally. During thermal stratification periods, the oxygenation of the sediment is inhibited, which leads to the exhaustion of sediment EAs (other than CO_2) by microbial processes (Bedard and Knowles 1991; Mattson and Likens 1993). In contrast, sediment oxygenation, which is induced by water-column mixing during spring and autumn, as well as by biological and physical turbation, activates the biogeochemical processes that regenerate the sediment EA pool. The increasing availability of EAs (other than CO_2) in sediments can mitigate CH_4 emissions in several ways. EAs can directly inhibit methanogenesis (Klüber and Conrad 1998) or decrease/suppress it by diverting the flow of electrons (from H_2, volatile fatty acids, alcohols) generated by fermentative bacteria from methanogenic to other anaerobic respiration pathways (Klüpfel *et al*. 2014). EAs can also increase CH_4 consumption via CH_4 oxidation (á Norði and Thamdrup 2014). However, Fe^{3+} and Mn^{4+} (generated via Fe^{2+} and Mn^{2+} oxidation), by means of reacting with OM, can also increase OM recalcitrance and protect it from microbial degradation (Lalonde *et al*. 2012; Estes *et al*. 2017). This could also suppress methanogenesis via decreasing the availability of methanogenic substrates. The recently reported Fe^{3+}-induced suppression of both CH_4 and CO_2 production in boreal lake sediments and peats (Karvinen, Lehtinen and Kankaala 2015) indeed implies that this process could play an important role in reducing CH_4 emissions from freshwater systems. It is well known that MO in oxic sediment layers represents an efficient CH_4 sink in lakes (Hanson and Hanson 1996) and that increased EA availability reduces methanogenesis in freshwater sediments (Segarra *et al*. 2013; Karvinen, Lehtinen and Kankaala 2015). However, the roles of the different EA-induced mechanisms that reduce methanogenesis (i.e. direct

inhibition, increased anaerobic respiration, or increased OM recalcitrance) and the effects of increased EA availability on AOM activity in freshwater sediments remain unclear.

In this study, we hypothesized that, in addition to aerobic MO, AOM, coupled with the reduction of Fe^{3+}, Mn^{4+}, NO_3^-, or SO_4^{2-}, takes place in boreal lake sediments. We further hypothesized that increased Fe^{3+} and Mn^{4+} decrease both CH_4 and CO_2 production in lake sediments via increasing OM recalcitrance and protection from microbial degradation. We conducted two sets of sediment slurry experiments with an increased concentration of either Fe^{3+}, Mn^{4+}, SO_4^{2-}, NO_3^-, or O_2 and analyzed the changes induced by the increase in each of the EAs in the potential rates of CH_4 oxidation and production and total inorganic carbon (TIC) production. Furthermore, the effects of the increased Fe^{3+} and Mn^{4+} availability on the structure of the bacterial and archaeal communities were assessed using next-generation sequencing (NGS) of the ribosomal 16S rRNA genes. The Fe^{3+} and Mn^{4+}-induced effects on the community structure and activity of methanogenic/methanotrophic archaea were also specifically studied by NGS of methyl-coenzyme M reductase (*mcrA*) genes and *mcrA* transcripts, respectively.

MATERIALS AND METHODS

Sediment sampling

The sediment samples for this study were collected from two sites in September 2012, namely a *Phragmites australis*-dominated littoral site (depth ca. 0.8 m) in a mesotrophic lake (L. Orivesi; 62º31'N, 29º22'E) and a profundal site (depth 7.5 m) in another mesotrophic lake (L. Ätäskö; 62°02N', 29°59'E). Samples from the profundal site were also obtained in June 2014. These two sites were selected due to previously determined background information, that is, high CH_4 emission rates were documented at the littoral site of L. Orivesi (Juutinen *et al*. 2003), while for L. Ätäskö, the postglacial sediment accumulation rate with ^{14}C-based depth-zone dating was

available (Pajunen 2004; Table 1). The water columns in the study sites are not thermally stratified during the open water season. Based on measurements taken during sampling in 2012, the water above the sediment at both sites was oxic (O_2 > 265 μmol L^{-1}). O_2 was not measured in 2014. However, open data available from the Finnish Environment Institute show that the water column of the profundal site is oxic until the bottom during the open water season. The uppermost samples, i.e. 0–10 cm (sample code is $P_{0\text{-}10}$) (six cores in 2012 and 10 cores in 2014) and 10–30 cm ($P_{10\text{-}30}$) (six cores in 2012 and 10 cores in 2014) layers at the profundal site and a 0–25 cm ($L_{0\text{-}25}$) (six cores in 2012) layer at the littoral site, were collected using a Kajak-type gravity corer (Ø = 54 mm). The deeper samples, 90–130 cm ($P_{90\text{-}130}$) (four cores in 2012) and 390–410 cm ($P_{390\text{-}410}$) (three cores in 2012) layers at the profundal site, were collected using a Livingston-type piston corer (Ø = 54 mm) (Table 1). Sediments were sectioned into depth layers and packed in gas-tight, sterile plastic bags already in the field, except for the sediment cores for $P_{390\text{-}410}$, which were sealed and transported to the laboratory as a whole. Sediments from the different cores were pooled for $P_{0\text{-}10}$, $P_{10\text{-}30}$, and $L_{0\text{-}25}$, whereas those for $P_{90\text{-}130}$ were not pooled but handled and packed individually. Contact with the air was minimized during the collection and handling procedures. Samples were transported to the laboratory on ice and covered from light.

In vitro incubations to determine the potential CH_4 oxidation and net production rates of CH_4 and total inorganic carbon (TIC)

Slurry preparation and incubation

The experimental setup consisted of testing the effects of different EAs and CH_2F_2 on CH_4 and TIC production and CH_4 consumption potentials (Table 2) as well as the determination of

potential Fe^{3+} and Mn^{4+} reduction (Table 3). Setting up the incubations took place in a glove bag under a N_2 gas flow. The cores for $P_{390-410}$ were first sectioned and put into sterile plastic bags, and similar to P_{90-130} samples, the sediments from the different cores were not pooled but handled individually. The middle parts of the sediments from the bags were collected for incubations, avoiding the outer sediment surfaces, which might have been exposed to air during sampling. The sediments were homogenized and weighted into N_2-flushed, pre-sterilized (by autoclaving) glass incubation bottles. In 2012, ~60 g of wet sediment from L_{0-25} and P_{10-30}, as well as ~50 g and ~40 g of sediment from P_{90-130} and $P_{390-410}$, respectively, were weighted into 150 ml bottles (12–16 bottles per sediment type, 59 bottles altogether). In 2014, wet sediment from the profundal site, ~50 g from P_{0-10}, and ~60 g from P_{10-30} was weighted into 300 ml bottles (38 and 40 bottles of P_{0-10} and P_{10-30}, respectively) (Table 2). Soon thereafter, the sediments obtained in 2014 were slurried by adding 50 ml O_2-free MQ-H_2O to each bottle, followed by brief, vigorous shaking. All bottles were then re-flushed with N_2 gas and closed with gas-tight caps and rubber septa. The sediments obtained in 2012 were pre-incubated to remove any traces of O_2 by storing them in the dark at a temperature of +4°C for seven days. Headspaces were then flushed with He (with three cycles of vacuum/He flushing). The sediments were slurried by the addition of O_2-free, sterilized artificial porewater (146 mM NaCl, 13.4 mM $MgCl_2$, 0.3 mM $CaCl_2$, 0.8 mM KCl, and 2.9 mM $NaHCO_3$) at a 1:2 ratio of porewater (V/w) to each bottle followed by brief, vigorous shaking.

The bottles containing the 2012 sediments were then divided into four treatments: (1) $^{13}CH_4$, (2) $^{13}CH_4$ + 2 mM SO_4^{2-} (as Na_2SO_4), (3) $^{13}CH_4$ + 2 mM NO_3^- (as $NaNO_3$), and (4) $^{13}CH_4$ + O_2, with three to four replicate bottles included in each treatment for each of the four sediment types (L_{0-25}, P_{10-30}, P_{90-130}, $P_{390-410}$). Replicates for P_{90-130} and $P_{390-410}$ represented the different

sampling cores. The bottles containing the 2014 sediments were divided into five treatments: (1) $^{13}CH_4$, (2) $^{13}CH_4$ + 10 mM Fe^{3+} [amorphous $Fe(OH)_3$; Lovley and Phillips 1986], (3) $^{13}CH_4$ + 10 mM Mn^{4+} (solid MnO_2; Lovley and Phillips 1988), (4) $^{13}CH_4$ + O_2, and (5) $^{13}CH_4$ + CH_2F_2, as well as five corresponding treatments with non-labelled CH_4, with three to four replicate bottles included in each treatment for both sediment types ($P_{0\text{-}10}$, $P_{10\text{-}30}$) (Table 2).

The *in situ* porewater concentrations of the EAs were not measured, except for the Mn concentration in $P_{0\text{-}10}$ (~27 μM), which is within the typical range (2–40 μM) reported in surface sediments of arctic lakes (Bretz and Whalen 2014). However, in the 0–2 cm surface sediment layer of a boreal (Finnish) high-NO_3^- lake (L. Pääjärvi, NO_3^- > 65 μM in the water above the sediment), the porewater NO_3^- concentration was previously found to only reach 14 μM during the growing season (Rissanen *et al.* 2013). The porewater SO_4^{2-} concentration typically ranges from ~20 to ~300 μM in the sediments of oligotrophic and mesotrophic lakes (Holmer and Storkholm 2001), while the porewater Fe concentration has been reported to only reach ~400 μM in previously studied northern lakes (Huerta-Diaz, Tessier and Carignan 1998; Bretz and Whalen 2014). This suggests that all EAs were added in significantly higher concentrations when compared to *in situ* conditions. Thus, this approach should show the effect of increased EA availability on the consumption and production of CH_4, as well as the TIC production processes, at the level of process potentials.

After preparing the EA amendments, all bottles in the anaerobic treatments (1 to 3 in 2012, 1 to 3 and 5 in 2014) were flushed with He (in 2012) or N_2 (in 2014), followed by the addition of He or N_2 overpressure, while the bottles in the aerobic treatments were treated similarly with air. The headspaces were then amended with 1 ml of non-labelled CH_4 (in 2014), 0.6 ml (in 2012), or 1 ml (in 2014) of ^{13}C-enriched CH_4 (^{13}C percentage was 8.2% in 2012 and

10.9% in 2014), followed by the addition of 0.5 ml of CH_2F_2 to treatment 5 in 2014 (headspace concentration ~0.25%). The ^{13}C-enriched CH_4 mixture was made by mixing CH_4 (99.95% purity, INTERGAS, UK) with $^{13}CH_4$ (99.5% purity, 99.9% ^{13}C, Cambridge Isotope Laboratories, Inc., USA) in an He-flushed, O_2-free glass bottle with NaOH powder to remove any contaminating CO_2. The bottles were taken from the glove bag and incubated in the dark at +4°C for up to 14 months in 2012, and at +10°C for up to four months in 2014. During the incubation period, the headspace concentration of CH_4 was measured five times in 2012 and four to five times in 2014, while those of the CO_2 and the ^{13}C content of CO_2 were measured six times in 2012 and four times in 2014.

CH_2F_2 inhibits CH_4 oxidation via its effect on methane mono-oxygenase (inhibited at a concentration > 0.03%). It also inhibits acetate-consuming methanogenesis (inhibited at a concentration > 0.1%; Miller, Sasson and Oremland 1998). Since ANME archaea use the H_2-consuming methanogenesis pathway in reverse (Timmers *et al*. 2017), it can be speculated that CH_2F_2 would inhibit CH_4 oxidation by MOBs and *NC 10* bacteria (since both use methane mono-oxygenase), but not AOM by ANME archaea. Furthermore, experiments conducted with *Methanosarcina acetivorans* suggest that TMO by acetate-consuming methanogens transfers methane-C to acetate, but not to CO_2 (Moran *et al*. 2007). As we did not measure acetate, TMO by acetate-consuming methanogens and its possible inhibition goes undetected in this study. Thus, the possible inhibition of CH_4 oxidation (to CO_2) by CH_2F_2 could specifically indicate MOB or *NC 10* bacteria activity during the incubations.

Determination of CH_4 and CO_2 concentrations and the isotopic composition of CO_2

The gas concentrations were measured in 2012 using an Agilent 6890N (Agilent Technologies, USA) gas chromatograph (GC) with an electron capture detector for CO_2 and a

flame ionization detector (FID) for CH_4 (first and second sampling), an Autosystem XL (Perkin Elmer, USA) GC with a thermal conductivity detector (TCD) for both gases (third sampling), an infrared Calanus gas analyzer (according to the method of Salonen 1981) for CO_2 (fourth to sixth sampling), an Agilent 6890N GC with a FID (fourth sampling), and a Clarus 500 (Perkin Elmer, USA) GC with a FID for CH_4 (sixth sampling). In 2014, the CH_4 and CO_2 concentrations were determined using a TurboMatrix and a Clarus 580 GC (Perkin Elmer, USA), a headspace sampler, and a GC equipped with a FID and a nickel catalyst for converting carbon dioxide to CH_4. The same standards were used each time.

The fractional abundance of ^{13}C in the CO_2 gas, ^{13}F,

$$^{13}F = \frac{^{13}\mathrm{C}}{(^{13}\mathrm{C} + {}^{12}\mathrm{C})} \qquad (1)$$

was analyzed with a Gasbench II (Thermo Fisher Scientific, Bremen, Germany), an online gas preparation and introduction system for isotope ratio mass spectrometry, coupled with a Delta Plus Advantage isotope ratio mass spectrometer (IRMS) (Thermo Fisher Scientific).

***In vitro* incubations to determine the reduction of Fe^{3+} and Mn^{4+}**

The Fe^{3+} and Mn^{4+} reduction incubations with samples from $L_{0\text{-}25}$ and $P_{0\text{-}10}$ in 2012 were set up similarly to the gas incubations described above. Approximately 9 g of wet sediment was slurried with 34 ml of N_2-flushed MQ-H_2O in 300 ml bottles (nine bottles from both $L_{0\text{-}25}$ and $P_{0\text{-}10}$), which were then divided into three treatments: (1) no additions, (2) 10 mM Fe^{3+}, and (3) 10 mM Mn^{4+}, with three replicate bottles included in each treatment for both sediment types (Table 3). Following the N_2 flushing, the bottles were taken from the glove bag and incubated in darkness at +10°C for 4.5 months. Slurry samples for the determination of the Fe^{3+} and Mn^{4+}

reduction were taken from the bottles through a septum eight times during the incubation period. The bottles were briefly shaken before each sampling.

The Fe^{3+} reduction activity was measured as Fe^{2+} production using a ferrozine-based assay (Lovley and Phillips 1986), as previously described by Karvinen, Lehtinen, and Kankaala (2015). The Mn^{4+} reduction activity was measured by the accumulation of soluble Mn^{2+}. The slurry samples were acidified (pH 2) with HCl and then centrifuged (4500 RPM, 15 min). The Mn concentration of the supernatant was measured using an AAnalyst 300 atomic absorption spectrophotometer (Perkin Elmer, USA).

Other analyses

The oxidation reduction potential (ORP) and pH of the sediment slurries collected in 2012 and 2014 were measured at the end of the incubations using a pH 3110 unit (WTW) equipped with a SenTix ORP electrode and a SenTix 41 pH electrode (WTW). In the 2012 experiment, pH was recorded at the start of the incubations, and a linear change in the [H+] was assumed for the whole incubation period in order to enable the TIC calculations (Table S1, Supporting Information). In 2014, pH and ORP changes were monitored alongside the incubations (measurements at four to five time points) using an additional batch of slurry samples, with one replicate per each treatment: (1) no amendments, (2) Fe^{3+}, (3) Mn^{4+}, (4) O_2, and (5) CH_2F_2 (Fig. S1, Supporting Information).

Dry weight (DW) of the sediments was analyzed by drying at 105 °C for 24 h. C and N contents of the sediment were measured from dry sediment using Thermo Finnigan Flash EA1112 elemental analyzer (Thermo Fisher Scientific). Total Fe content of the sediments was determined as in Karvinen, Lehtinen, and Kankaala (2015). Total Mn content of the sediment

supernatant (pH 2) was determined as explained above for the Mn^{4+} reduction analyses (Table 1).

Calculations

The concentration of CH_4 and CO_2 dissolved in the slurry phase of the incubation bottles was calculated from their partial pressures in the gas phase (headspace) using Henry's law. This allowed for the calculation of the total amount of CH_4 in the incubation bottles (gas phase + slurry phase). The amount of bicarbonate dissolved in the slurry phase was calculated from the amount of dissolved CO_2 using the dissociation constant of bicarbonate (Stumm and Morgan 1981) and the pH of the sediment slurries (see above). The total inorganic carbon (TIC) was defined as the sum of bicarbonate, gaseous, and dissolved CO_2. The potential net production rates of CH_4 and TIC, as well as the production rates of Fe^{2+} (potential Fe^{3+} reduction) and Mn^{2+} (potential Mn^{4+} reduction), were measured for each incubation bottle as a linear increase in the total amount of these substances with time.

Potential CH_4 oxidation was measured for each incubation bottle as a linear increase in the amount of CH_4 oxidized with time. This was calculated for each time point using a modification of the equation used by Blazewicz *et al*. (2012) and Moran *et al*. (2005):

$$\mathrm{N_{oxCH4}} = [(^{13}F_{\mathrm{L}} - {}^{13}F_{\mathrm{n}}) \times N_{\mathrm{LTIC}}] \times \frac{(N_{\mathrm{iCH4}} + N_{\mathrm{bCH4}})}{(F_{\mathrm{iCH4}} N_{\mathrm{iCH4}} + F_{\mathrm{bCH4}} N_{\mathrm{bCH4}})} \qquad (2)$$

where N_{oxCH4} is the amount of CH_4 oxidized in the incubation bottle, N_{LTIC} is the amount of TIC in the incubation bottle with the added $^{13}CH_4$, N_{iCH4} is the amount of CH_4 initially in the incubation bottle (day 1), N_{bCH4} is the amount of biogenic CH_4 produced during incubation, F_{iCH4} is the initial fractional abundance of ^{13}C in CH_4 (same as the ^{13}C-label percentage, see above),

F_{bCH4} is the fractional abundance of ^{13}C in biogenically produced CH_4, $^{13}F_L$ is the fractional abundance of ^{13}C in the CO_2 in the incubation bottle with the added $^{13}CH_4$, while $^{13}F_n$ is the fractional abundance of ^{13}C in the CO_2 in the incubation bottle of the respective treatment with the added non-labelled CH_4 (for the 2014 incubations) or the fractional abundance of ^{13}C in the CO_2 initially in the incubation bottle with added $^{13}CH_4$ (for the 2012 incubations). The left side of the equation (left from the central multiplication [x] sign) estimates the amount of $^{13}CO_2$ produced from the added $^{13}CH_4$ for each time point, which is multiplied by the right side of the equation estimating the ratio of total CH_4 to ^{13}C-CH_4. Both the $^{13}F_L$ and $^{13}F_n$ were determined using IRMS (from the gas phase CO_2), while the N_{LTIC} and N_{iCH4} were determined using GC (see above). The N_{bCH4} was calculated as the difference between the total amount of CH_4 at a given time point and the N_{iCH4}. The effects of the isotopic fractionation associated with CO_2 dissolution and bicarbonate formation (Stumm and Morgan 1981) were considered to be negligible in the calculations, since the incubations were labelled with ^{13}C. The CH_4 oxidation in this study was determined solely based on the transfer of ^{13}C from CH_4 to TIC, and hence, the proportion of CH_4-C bound to the biomass was not taken into account. As in the study by Blazewicz *et al*. (2012), it was assumed that the biogenic CH_4 produced during the incubation had $\delta^{13}C$ = -50‰ (F_{bCH4} = 0.01051). The chosen value represents the typical values of boreal lakes, since it is in the middle of the total range, -20‰ to -81‰, as measured previously from the water columns of two boreal lakes (Kankaala *et al*. 2007; Nykänen *et al*. 2014). All the process rates were expressed as per gram of dry weight and per cm^3 of wet sediment.

Molecular analyses

In 2012, 15 ml of wet sediment taken from L_{0-25}, P_{0-10} and P_{10-30} prior to the incubations was stored at -20°C and subsequently freeze-dried for molecular analyses. In 2014, ~500 mg

sediment aliquots were taken for molecular analyses from $P_{0\text{-}10}$ and $P_{10\text{-}30}$ prior to the incubations and from the sediment slurry of the treatments after the incubations and then stored at -80°C. DNA was extracted from the freeze-dried sediment collected in 2012 using the PowerSoil DNA isolation kit (MOBIO). In 2014, DNA and RNA were simultaneously extracted from the frozen sediment samples using the method of Griffiths *et al*. (2000).

General microbial communities were studied by NGS of bacterial and archaeal 16S rRNA gene amplicons. Furthermore, potential and active methanogenic/methanotrophic archaea were specifically studied by NGS of *mcrA* from DNA and mRNA, respectively. Primer pairs utilized for PCR amplification of the 16S rRNA gene were Arch340F (5'-CCCTAYGGGGYGCASCAG-3')/Arch1000R (5'-GGCCATGCACYWCYTCTC-3') (Gantner *et al.* 2011) for archaea and 27F (5'-AGAGTTTGATCMTGGCTCAG)/338R (5'-TGCTGCCTCCCGTAGGAGT-3') for bacteria, while those utilized for PCR amplification of the *mcrA* gene were *mcrA* forward (5'-GGTGGTGTMGGATTCACACAR-3')/*mcrA* reverse (5'-TCATTGCRTAGTTWGGRTAGTT-3') (Beal, House and Orphan 2009). PCR of 16S rRNA and *mcrA* genes, reverse-transcriptase PCR (RT-PCR) of *mcrA*, preparation of sequence libraries as well as sequencing (Ion Torrent™ Personal Genome Machine) are described in detail in Supplemental Methods (Supplemental Methods 1, Supporting Information).

Mothur (Schloss *et al*. 2009) was used in all subsequent sequence analyses unless otherwise reported. The barcodes and primer sequences, as well as low-quality sequences (containing sequencing errors in the primer or barcode sequences, ambiguous nucleotides, and homopolymers longer than eight nucleotides), were removed. Framebot (FunGene website, http://fungene.cme.msu.edu/FunGenePipeline; Wang *et al*. 2013) was used to correct frameshift errors in the *mcrA* reads. The 16S rRNA gene sequences were assigned to taxonomies with a

naïve Bayesian classifier (bootstrap value cut off = 75%) (Wang *et al*. 2007) using the Greengenes database, which was amended by sequences of the recently described archaeal phyla *Verstraetearchaeota* presented in Vanwonterghem *et al*. (2016). Unclassified sequences as well as the sequences classified as chloroplasts, mitochondria, and eukaryota were removed. Furthermore, the bacterial sequences were removed from the archaeal libraries and *vice versa*. The taxonomic assignment for *mcrA* sequences was done similarly to the procedure for the 16S rRNA sequences, albeit with a custom-made database, whose preparation is described in Supplemental Methods (Supplemental Methods 2).

The 16S rRNA gene sequences were aligned using Silva reference alignment (Release 119), while the alignment of the *mcrA* sequences was conducted using a set of aligned *mcrA* sequences retrieved from the FunGene website (http://fungene.cme.msu.edu/hmm_detail.spr?hmm_id=16). Chimeric sequences, denoted using Mothur's implementation of Uchime (Edgar *et al*. 2011), were removed from the data. In addition, Schloss, Gevers and Westcott's (2011) modification of the Huse *et al*. (2010) pre-clustering algorithm was used to reduce the effect of potential sequencing errors. After these steps, the final datasets from the years 2012/2014 contained 24013/212584 (length = ~307 bp), 23507/77038 (~223 bp), and 2167/82818 (~263 bp) bacterial 16S rRNA gene, archaeal 16S rRNA gene, and *mcrA* sequence reads, respectively.

The sequences were divided into operational taxonomic units (OTUs) at 97% and 96% similarity levels for the 16S rRNA and *mcrA* genes, respectively. For the beta-diversity and taxonomic analyses, rare OTUs, that is, OTUs with ≤ 26 and ≤ 37 of 16S rRNA and *mcrA* sequences, respectively, were removed (thus, those OTUs with less than one sequence per sample on average were removed). Each sample was subsampled to the size of the smallest

sample (=3580/4223 bacterial and 4541/1123 archaeal 16S rRNA gene reads and 479/1180 *mcrA* reads per sample in the 2012/2014 datasets, respectively). The OTUs were assigned consensus taxonomies. In addition, a phylogenetic tree analysis was performed to further validate and fine-tune the classification of the *mcrA*-OTUs (Supplemental Methods 3 and Fig. S2, Supporting Information).

The bacterial and archaeal OTUs were classified into functional groups. For the archaea, these were: (1) acetate, (2) $H_2 + CO_2$, (3) methyl compound (Nazaries *et al*. 2013), (4) H_2 + methyl compound consuming methanogens (Borrel *et al*. 2013; Vanwonterghem *et al*. 2016), and (5) anaerobic methanotrophic archaea (Knittel and Boetius 2009). For the bacteria, the functional groups were: (1) fermentative (fermentative and syntrophic bacteria) (Herlemann *et al*. 2009; Yamada and Sekiguchi 2009; Kallistova, Goel and Nozhevnigova 2014; Wasmund *et al*. 2014; Wrighton *et al*. 2014; Zheng *et al*. 2016), (2) Fe^{3+}/Mn^{4+}-reducing (Finneran, Johnsen and Lovley 2003; Lovley 2006), (3) aerobic methanotrophic (Chowdhury and Dick 2013), and (4) anaerobic methanotrophic bacteria (Ettwig *et al*. 2010). Furthermore, representative 16S rRNA gene sequences of the *MCG* OTUs were searched against a *MCG* database consisting of the sequences of putative methanogens (Evans *et al*. 2015) and sequences classified into previously defined *MCG* sub-groups (Lazar *et al*. 2015) using BLASTN (Altschul *et al*. 1990).

The sequencing data were deposited into the NCBI's Sequence Read Archive (Study accession SRP091914).

Statistical analyses

Differences in the process rate variables, the relative abundance of the functional groups of bacteria and archaea, and the relative activity (relative *mcrA* transcript abundance) of the functional groups of methanogenic/methanotrophic archaea among the treatments were tested for

each sediment layer using a t-test or one-way ANOVA. When necessary, the variables were log10 transformed to fulfil the ANOVA assumptions. The one-way ANOVA was followed by pair-wise post-hoc tests using the least significant difference (LSD) technique with Hochberg-Bonferroni-corrected α-values. The correlations among the relative activity of the functional groups of archaea and the process rates were tested using Spearman's rank correlation analysis. The ANOVA, t-tests, and correlation analysis were conducted using IBM SPSS Statistics version 23.

Variations in the beta diversity (Bray-Curtis distance metric) were visualized by non-metric multidimensional scaling (NMS) and tested among the treatments using a one-way permutational multivariate analysis of variance (PerMANOVA) (Anderson 2001; McArdle and Anderson 2001). The NMS was conducted using PC-ORD version 6.0 (MjM Software, Gleneden Beach, Oregon, USA) (McCune and Mefford 2011). The PerMANOVA was conducted using PAST version 3.06 (Hammer, Harper and Ryan 2001). Furthermore, differences in the abundance of each OTU among the treatments were tested using Mothur's implementation of the linear discriminant analysis (LDA) effect size (LEfSe) method (Segata *et al*. 2011).

RESULTS

Potential net production rates of CH_4 and TIC and the potential CH_4 oxidation

The potential net production rates of CH_4 and TIC in anaerobic conditions ranged from 0.6 to 82.5 nmol CH_4 g^{-1}_{DW} d^{-1} (0.1–11.7 nmol CH_4 cm^{-3} d^{-1}) and from 19.7 to 318.7 nmol TIC $g^{-1}_{DW}d^{-1}$ (3.0–45.1 nmol TIC cm^{-3} d^{-1}), respectively (Table 2). They were one order higher at the littoral site than at the profundal site (when compared in 2012), and also differed among the depth layers at the profundal site (Table 2). There were differences between the 2012 and 2014 rates, which

were likely caused by the different incubation setups (see the Materials and Methods section), and hence, are not considered further. The major focus in this study was on the effects of increased EAs and CH_2F_2, that is, on the differences between the CH_4 treatment only and the other treatments (CH_4 + EAs and CH_4 + CH_2F_2) (Table 2).

The addition of Fe^{3+} and Mn^{4+} decreased the potential net CH_4 production by 30% and 77% in $P_{0\text{-}10}$, respectively. In $P_{10\text{-}30}$, the addition of Fe^{3+} did not decrease it statistically significantly, although the addition of Mn^{4+}, NO_3, and SO_4^{2-} decreased it by 83%, 60%, and 60%, respectively (Table 2). In contrast, NO_3^- and SO_4^{2-} did not affect net CH_4 production in the deeper layers, $P_{90\text{-}130}$ and $P_{390\text{-}410}$, at the profundal site (Table 2). The addition of SO_4^{2-} and NO_3^- also decreased the potential net CH_4 production by 66% and 40% in $L_{0–25}$ (Table 2), respectively. The addition of Fe^{3+} and Mn^{4+} also reduced the potential net TIC production by 60% and 42% in $P_{0–10}$, respectively, although none of the added anaerobic EAs affected it in the other layers of the profundal site, nor at the littoral site (Table 2). The potential net CH_4 and TIC production rates were generally similar between the CH_4 and CH_4+CH_2F_2 treatments (Table 2). However, during the first week of incubation, CH_2F_2 inhibited CH_4 production in two out of six and three out of eight incubation bottles containing sediment from $P_{0–10}$ and $P_{10–30}$, respectively (Figs. S3A and C, Supporting Information). The relative expression of the *mcrA* (relative abundance of *mcrA* transcripts) of the acetate-consuming methanogens decreased with the increasing potential net CH_4 production ($\rho = -0.709$, $p < 0.05$), whereas no other correlations between the *mcrA* expression of the archaeal functional groups and the potential net production rates of CH_4 and TIC were detected.

The addition of O_2 generally resulted in the highest potential net TIC production. It also led to CH_4 consumption, except for the deepest layer, $P_{390–410}$, of the profundal site, where no

CH_4 production or consumption occurred (Table 2). ^{13}C labelling confirmed that the CH_4 consumption was due to aerobic CH_4 oxidation ranging from 0 to 49.3 nmol g^{-1}_{DW} d^{-1} (0–7.0 nmol cm^{-3} d^{-1}) and also varying between sites (when compared in 2012) and depth layers (Table 2). The potential CH_4 oxidation in the anaerobic incubations ranged from 0 to 2.1 nmol g^{-1}_{DW} d^{-1} (0–0.3 nmol cm^{-3} d^{-1}). It was not affected by the addition of NO_3^-, SO_4^{2-}, Fe^{3+}, or Mn^{4+} at the profundal site, although NO_3^- and SO_4^{2-} suppressed it at the littoral site (Table 2). The potential CH_4 oxidation did not generally differ between the CH_4 and CH_4+CH_2F_2 treatments (Table 2). However, during the first week of incubation, CH_2F_2 inhibited it in two out of three and two out of four incubation bottles containing sediment from $P_{0–10}$ and $P_{10–30}$, respectively (Figs. S3B and D). The potential CH_4 oxidation activity in the anaerobic treatments increased as the net TIC production increased ($\rho = 0.524$, $p < 0.05$), but it was not correlated with the net CH_4 production rate, nor with the relative expression of *mcrA* of the functional groups of archaea.

Potential rates of Fe^{3+} and Mn^{4+} reduction

The natural concentrations of Fe and Mn were higher in P_{0-10} than in L_{0-25} (Table 1). The average potential Fe^{3+} and Mn^{4+} reduction rates ranged from 16.1 to 913.3 nmol $g^{-1}_{DW}d^{-1}$ (3.3–129.1 nmol cm^{-3} d^{-1}) and 13.5 to 1066.4 nmol $g^{-1}_{DW}d^{-1}$ (2.8–221 nmol cm^{-3} d^{-1}), respectively. The natural (non-amended) rate of anaerobic Fe^{3+} reduction was considerably higher in P_{0-10} than in L_{0-25}, whereas the natural Mn^{4+} reduction was only slightly higher in P_{0-10} (Table 3). As expected, the addition of Mn^{4+} increased the Mn^{4+} reduction rate significantly at both sites (Table 3). Further, the addition of Fe^{3+} increased the Fe^{3+} reduction rate significantly in L_{0-25}, although a much smaller increase was observed in P_{0-10} (Table 3).

Since the Fe^{3+} and Mn^{4+} reduction assays conducted in P_{0-10} were performed in similar conditions to the gas production/consumption incubations conducted in 2014, the contribution of

Fe^{3+} and Mn^{4+} reduction to C mineralization could be roughly estimated by assuming a 4:1 ratio for Fe^{3+} reduction:TIC production and 2:1 for Mn^{4+} reduction:TIC production (Hiscock and Bense 2014). The natural (non-amended) Fe^{3+} and Mn^{4+} reduction contributed to 63.4% and 3.5% of TIC production, respectively. However, when Fe^{3+} and Mn^{4+} were added, OM oxidation coupled with dissimilatory Fe^{3+} and Mn^{4+} reduction would have produced two to three times more TIC than was observed. This indicates that a large part of the Fe^{3+} and Mn^{4+} reduction in the Fe^{3+}- and Mn^{4+}-amended treatments was not coupled with the processes that produce TIC.

Microbial community structure

The sample storage and DNA extraction methods differed between the study years (see Materials and Methods), which precludes comparisons of microbial composition between 2012 and 2014. The structure of the microbial communities differed between the littoral and profundal sites and between $P_{0–10}$ and $P_{10–30}$ at the profundal site (Figs. 1 and 2, Figs. S4, S5, and S6, Supporting Information). Methanogens dominated the archaeal community at the littoral site, while their contribution was lower at the profundal site (Fig. 1A). *Methanobacteriaceae* that consume H_2+CO_2 were more abundant at the littoral site than at the profundal site, whereas an opposite pattern was observed for acetate-consuming *Methanosaetaceae* and H_2+CO_2-consuming *Methanoregulaceae* (Fig. 1). The other detected but less abundant methanogenic groups were H_2+CO_2-consuming *Methanocellales* and H_2+methyl-compound-consuming *Methanomassiliicoccales* and *Verstraetearchaeota* (Fig. 1). The anaerobic methane-oxidizing archaea all belonged to the ANME-2D archaea and were present in low abundance (0.02–3.4% of archaeal 16S rRNA and 0–3.9% of *mcrA* gene sequences) (Fig. 1). They had a higher relative abundance at the profundal site, especially in P_{10-30} (Fig. 1). Of the methanogenic archaea actively expressing their *mcrA* gene in P_{0-10}, *Methanosaetaceae* and *Methanoregulaceae* were

dominant, followed by *Methanobacteriaceae* (Fig. 1B), with much less of a contribution from *Methanomassiliicoccales* (2–4% of *mcrA* transcripts) and *Verstraetearchaeota* (0.1–0.4% of *mcrA* transcripts). Based on the much higher relative abundance of their *mcrA* at the mRNA level than at the DNA level, the ANME-2D archaea were especially active in the non-incubated sample (12% of *mcrA* transcripts), while their *mcrA* expression decreased considerably during the incubations (2.5–4.5% of *mcrA* transcripts after incubations) (Fig. 1B). Of the other archaea, the *MCG* archaea dominated at both sites, with less of a contribution from *Parvarchaea* and *DHVEG-1* (a family within *Thermoplasmata*) (Fig. S4). The *MCG* OTUs were not closely affiliated with the putative methanogenic/methanotrophic *MCG* (Evans *et al*. 2015) and mainly belonged to the *MCG* subgroups 6, 1, 15, 7/17, and 11 (based on Lazar *et al*. 2015).

Bacteroidetes, *Chloroflexi*, and *Deltaproteobacteria* (*Desulfobacteraceae*, *Syntrophaceae*, *Syntrophobacteraceae*, *Syntrophorhabdaceae*) dominated the putative fermentative bacterial community at both sites, while the other putative fermentative bacteria belonging to *Clostridia*, *Microgenomates*, *SR 1*, *TM 6*, *Saccharibacteria*, *Elusimicrobia*, and *Parcubacteria* constituted a much smaller segment of the bacterial community (Fig. 2A). Of the putative Fe^{3+}/Mn^{4+}-reducing bacteria, *Geobacter* dominated, with a lower contribution from *Thiobacillus* and *Geothrix.* The Fe^{3+}/Mn^{4+}-reducing bacteria were generally found with a very low abundance (≤ 1.1%), except in the CH_4+Fe^{3+} and CH_4+Mn^{4+} treatments in $P_{10\text{-}30}$, in which the *Geobacter* were enriched (up to 5.9%) (Fig. 2B). The methanotrophic bacterial community consisted of *Methylococcales*, *Methylocystacea*, and *Methylacidiphilae* (Fig. 2C). As was the case with the ANME-2D archaea, the putative anaerobic methanotrophic bacteria within the *NC 10* phyla were present with a low relative abundance (0.1–0.5%) and were also more abundant at the profundal site (Fig. 2C).

Based on the analyses at the DNA level, the general and *mcrA*-carrying archaeal community did not differ among the CH_4, CH_4+Fe^{3+}, and CH_4+Mn^{4+} treatments after the incubations (PerMANOVA, $p > 0.05$). In addition, the relative abundance of the functional groups of archaea did not differ among the treatments (one-way ANOVA, $p > 0.05$) (Fig. 1). Yet, according to the LEfSe analyses, some acetate-consuming *Methanosaetaceae* OTUs were more abundant in either the CH_4+Fe^{3+} or CH_4+Mn^{4+} treatments, while one H_2+CO_2-consuming *Methanoregulaceae* OTU, based on the 16S rRNA gene, exhibited its highest relative abundance in the CH_4 treatment in $P_{0\text{-}10}$ (Figs. S7 and S8, Supporting Information). One H_2+methyl-compound-consuming *Verstraetearchaeota* OTU, based on the 16S rRNA gene, exhibited its highest relative abundance in the CH_4+Fe^{3+} treatment in $P_{0–10}$, while two H_2+CO_2-consuming *Methanomicrobiales* OTUs, based on the *mcrA* gene, exhibited their highest relative abundance in the CH_4+Mn^{4+} treatment in $P_{10–30}$ (Figs. S7 and S8). Only one ANME-2D OTU, based on the *mcrA* gene, exhibited its highest relative abundance in the CH_4+Mn^{4+} treatment in $P_{10–30}$ (Fig. S8).

In contrast to the analyses at the DNA level, the relative *mcrA* expression of the different *mcrA*-carrying archaeal OTUs (mRNA level) differed between the CH_4 and CH_4+Mn^{4+} treatments (PerMANOVA, $p < 0.05$) (Fig. S6E). In addition, the relative *mcrA* expression of the H_2+methyl-compound-consuming methanogens was lower in the CH_4+Fe^{3+} treatment than in the other treatments (one-way ANOVA, $p < 0.05$), while the *mcrA* expression of the other functional groups did not differ among the treatments (one-way ANOVA, $p > 0.05$) (Fig. 1B). However, all the *mcrA* OTUs that exhibited their highest relative activity in the CH_4 treatment were H_2 consumers (Fig. 3A). In contrast, the relative expression of *mcrA* of one acetate-consuming *Methanosaetaceae* OTU was higher in the CH_4+Fe^{3+} and CH_4+Mn^{4+} treatments than in the CH_4

treatment (Fig. 3B). Only one H_2+CO_2 – consuming *Methanoregulaceae* OTU had its highest relative activity in CH_4+Mn^{4+} - treatment (Fig. 3C). The relative *mcrA* expression of the ANME-2D OTUs did not differ among the treatments.

In contrast to the archaea, the overall bacterial community differed between all three treatments in $P_{0–10}$ (PerMANOVA, $p < 0.05$), while the CH_4+Mn^{4+} treatment differed from the other treatments in $P_{10–30}$ ($p < 0.05$) (Figs. S6A and B). In addition, the relative abundance of the fermentative bacteria was higher in the CH_4+Mn^{4+} treatment than in the CH_4+Fe^{3+} treatment in $P_{0–10}$ (one-way ANOVA, $p < 0.05$), while the metal-reducing bacteria differed in their relative abundance between treatments in $P_{10–30}$, with the highest relative abundance being seen in the CH_4+Mn^{4+} treatment, the second highest in the CH_4+Fe^{3+} treatment, and the lowest in the CH_4 treatment (Figs. 2A and B). Neither the MOBs, nor the *NC 10* bacteria differed in their relative abundance between the treatments. There were, however, considerable differences in the responses of the OTUs to the treatments between the depth layers (Fig. 4). In $P_{10–30}$, the OTUs that exhibited their highest abundances in the CH_4+Fe^{3+} and CH_4+Mn^{4+} treatments were mostly *Geobacter* and, for the CH_4+Fe^{3+} treatment, the *WS3* group (Figs. 4E and F). In contrast, in $P_{0–10}$, the OTUs that had their highest abundance in the CH_4+Fe^{3+} and CH_4+Mn^{4+} treatments were mostly *Chloroflexi*, for the CH_4+Fe^{3+} treatment, *Betaproteobacteria*, and for the CH_4+Mn^{4+} treatment, *Elusimicrobia* (Figs. 4B and C). Of the known sulfur-cycling bacteria, one OTU within *Desulfobulbaceae* exhibited its highest abundance in the CH_4+Mn^{4+} treatment in $P_{0–10}$ (Fig. 4C).

DISCUSSION

CH_4 oxidation

The potential CH_4 oxidation in the anaerobic incubations was not enhanced by the increased availability of EAs, which contradicts our hypothesis that AOM coupled with the reduction of Fe^{3+}, Mn^{4+}, NO_3^-, or SO_4^{2-} would occur within the studied boreal lake sediments. The potential anaerobic CH_4 oxidation (0–0.3 nmol cm^{-3} d^{-1}) in the two investigated lakes was also very low when compared to those measured from other freshwater systems, including lakes (0–44 nmol cm^{-3} d^{-1}; Sivan *et al*. 2011; á Norði, Thamdrup and Schubert 2013; Deutzmann *et al*. 2014), nitrate-enriched pond microcosms (43–400 nmol cm^{-3} d^{-1}; á Norði and Thamdrup 2014), and wetland sediments (~0–30 nmol $cm^{-3}d^{-1}$; Segarra *et al*. 2013). It was only up to 2.5% of the maximum potential net CH_4 production (treatments amended with only CH_4), whereas the aerobic MOBs could consume up to 60% of the maximum potential net CH_4 production.

CH_4 oxidation in anaerobic conditions can be mediated through AOM or TMO (Timmers *et al*. 2016). The independency of the potential CH_4 oxidation from the net potential CH_4 production in anaerobic conditions would suggest that CH_4 oxidation mainly took place through AOM at the profundal site. In contrast, the concurrent EA-induced decrease in the potentials of both CH_4 oxidation and net CH_4 production would suggest that CH_4 oxidation mainly took place through TMO at the littoral site (Table 2) (Moran *et al*. 2005; Meulepas *et al*. 2010; Timmers *et al*. 2016). However, the results of the CH_2F_2 experiments necessitate a more in-depth discussion of the contribution of the different processes to CH_4 oxidation.

In the headspace concentrations used in this study (0.25%), CH_2F_2 inhibits both methane mono-oxygenase and acetate-consuming methanogenesis (Miller, Sasson and Oremland 1998). Furthermore, CH_2F_2 is rapidly depleted after only a few days of incubation, leading to the recovery of the inhibited processes (Miller, Sasson and Oremland 1998; Vicca *et al*. 2009), which agrees with our finding that CH_2F_2-induced inhibition of the CH_4 processes only took

place during the first week of incubation. Since ANME archaea use the H_2+CO_2-consuming methanogenesis pathway in reverse (Timmers *et al*. 2017), it can be speculated that their activity would not be inhibited by CH_2F_2. As NO_3^-, which is also rapidly reduced to NO_2^- in anoxic sediments, did not enhance CH_4 oxidation, it can be suggested that the CH_2F_2-induced inhibition of the potential CH_4 oxidation was not due to the inhibition of NO_2^- using *NC 10* bacteria, but rather due to the inhibition of aerobic MOBs. Indeed, a risk of minor O_2 contamination from the substrate/tracer injection or due to diffusion from the rubber septa or silicon sampling ports during incubations, which could induce microaerobic CH_4 oxidation, has been acknowledged in previous incubation studies of anoxic freshwater samples (Blees *et al*. 2014; á Norði and Thamdrup 2014). It is, therefore, possible that the diffusion of trace amounts of O_2 from the septa during the incubation period could not be fully prevented in this study, either. Although the observed net CH_4 production and the measurements of ORP confirmed that anaerobic conditions, which are optimal for AOM, prevailed (Table S1, Fig. S1), it is possible that some active MOBs that used the trace O_2 were present on the surfaces of the sediment slurries. Thus, the inhibition of CH_4 oxidation by CH_2F_2 might indicate that besides AOM and TMO, MO could also have at least partially contributed to the CH_4 oxidation. Therefore, our potential anaerobic CH_4 oxidation rates could be better considered as overestimates, rather than underestimates, due to the possible contribution of MO. The possible MO activity also makes it impossible to separate TMO and AOM using the aforementioned criteria regarding the dependency between CH_4 production and oxidation (Meulepas *et al*. 2010).

The relative abundance of anaerobic CH_4 oxidizing bacteria (*NC 10*) and archaea (ANME-2D) was low, and neither their relative abundance, nor the relative abundance of the mRNA transcripts of ANME-2D was generally affected by increased Fe^{3+} or Mn^{4+}. Although

ANME-2D is generally found in various types of freshwater ecosystems (Welte *et al*. 2016), including lake sediments (L. Cadagno; Schubert *et al*. 2011), no comparable studies concerning its relative abundance in lake sediments exist. The relative abundance of *NC 10* bacteria (0.1–0.5% of bacteria) in the study lakes was within the same range (0.1–0.7 %) reported for aquaculture pond sediments, but it was lower than that measured from the sediments of a freshwater reservoir (1.0–1.5%) (Shen *et al*. 2016). In L. Constance, the relative abundance of *NC 10* bacteria was within the same range at a 12 m depth (~0–0.2%), but was substantially higher at ~80 m deep profundal depths (0.8–6.2%), where active NO_3^-/NO_2^--driven AOM was detected as well (Deutzmann *et al*. 2014). The MOB also substantially outnumbered the *NC 10* in our study, whereas the opposite was true in the profundal sediments of L. Constance (Deutzmann *et al*. 2014). However, due to possible bias in reducing the *NC 10* sequences when using universal 16S rRNA gene primers (Ettwig *et al*. 2009), the relative abundance of the *NC 10* bacteria may be underestimated in our study. Our data do not allow for a direct comparison between the numbers of ANME-2D archaea and MOBs. However, the total abundance of bacteria was more than ten times higher than that of archaea in previously studied lake sediments (Chan *et al*. 2005; Conrad *et al*. 2007; Conrad *et al*. 2010; Borrel *et al*. 2012), which strongly suggests that the ANME-2D archaea were substantially outnumbered by the MOBs in our study.

Taken together, these results indicate that anaerobic CH_4 oxidation is not important in mitigating CH_4 emissions from the investigated lakes. This finding contrasts with previously studied freshwater sediments, where the volumetric AOM rates were >15% of the CH_4 production rates or even larger than the CH_4 production (Sivan *et al*. 2011; á Norði, Thamdrup and Schubert 2013; Segarra *et al*. 2013; á Norði and Thamdrup 2014). Thus, anaerobic CH_4 oxidation can consume a substantial part of diffusive CH_4 flux before it reaches the sediment-

water interface (á Norði, Thamdrup and Schubert 2013; Deutzmann *et al*. 2014; á Norði and Thamdrup 2014). However, apart from the 4.5 m depth in the iron-rich L. Ørn (á Norði, Thamdrup and Schubert 2013), lake sediment AOM activity has been detected from sites that are deeper and, therefore, probably more environmentally stable than our study sites, for instance, from a 37 m depth in L. Kinneret (Sivan *et al*. 2011) and a ~80 m depth in L. Constance (Deutzmann *et al.* 2014), as well as from a nitrate-enriched stable pond sediment microcosm (á Norði and Thamdrup 2014). Furthermore, AOM organisms (*NC 10* bacteria) were much more abundant in deep profundal sediments (at > 40 m and 80 m depths) than in shallower sites in L. Biwa and L. Constance, respectively (Kojima *et al.* 2012; Deutzmann *et al.* 2014), as well as in the sediments of a large reservoir than in small ponds (Shen *et al*. 2016). Accordingly, the higher abundance of AOM organisms at the profundal study site compared with the littoral study site is probably due to its greater depth. Thus, a plausible explanation for the discrepancy between our study and previous lake AOM studies could be variations in ecosystem stability, since slow-growing AOM microbes require stable environmental conditions for growth and to maintain their populations (Deutzmann *et al*. 2014).

Previous studies of ANME-2D archaea enrichment cultures have shown their potential to use NO_3^- (Haroon *et al*. 2013; Ettwig *et al*. 2016), Fe^{3+}, and Mn^{4+} (Ettwig *et al*. 2016) as EAs in anaerobic CH_4 oxidation, while *NC 10* bacteria use NO_2^- (Ettwig *et al*. 2010). Environmental studies also suggest that ANME-2D are involved in SO_4^{2-}-dependent AOM (Timmers *et al*. 2016, 2017). However, our results showed that AOM organisms did not use inorganic EAs in the study sediments. We acknowledge that Fe^{3+} and Mn^{4+} (but not SO_4^{2-} and NO_3^-) were the only EAs tested with the anaerobic samples from $P_{0–10}$ (Table 2). However, as the ANME-2D archaea had a higher relative abundance in $P_{10–30}$, where the whole set of inorganic EAs were tested, the

possible effects of the EAs would have been even more likely to be detected. In addition, the *mcrA* expression of the ANME-2D was high *in situ* in $P_{0–10}$, and it decreased during the incubations, irrespective of the treatment. This suggests that exhaustion of some important substrate other than CH_4 or inorganic EAs took place during the incubations. This could actually imply that ANME-2D archaea utilized organic EAs (e.g. humic compounds), which were not tested in this study. Despite organic EAs being very likely generated by the reduction of Mn^{4+} or Fe^{3+} (Lovley *et al*. 1996; Kappler *et al*. 2004) during the incubations, their quantity or quality (e.g. oxidation stage) was probably not sufficient to support AOM. Alternatively, it can be speculated that ANME-2D archaea did not drive AOM, but instead performed methanogenesis in the investigated sediments. Yet, previously studied ANME-2D archaea were not capable of methanogenesis (Ding *et al*. 2016; Timmers *et al*. 2017). More studies are definitely needed to reveal the metabolic capabilities of different ANME-2D species.

Production of CH_4 and TIC

In contrast to the potential CH_4 oxidation, the potential net CH_4 production rates (0.6–82.5 nmol $g^{-1}{}_{DW}d^{-1}$; 0.1–11.7 nmol cm^{-3} d^{-1}) in the anaerobic incubations of the sediment slurries from the study lakes fell well within the range of reported CH_4 production rates in previous lake sediment studies: ~0–312 nmol $g^{-1}{}_{DW}$ d^{-1} (Schulz, Matsuyama and Conrad 1997; Marotta *et al*. 2014; Karvinen, Lehtinen and Kankaala 2015) and ~1–23 nmol cm^{-3} d^{-1} (Sivan *et al*. 2011; á Norði, Thamdrup and Schubert 2013). The potential net CH_4 production rates also well represent the magnitude and variation of the estimated potential gross CH_4 production rates, since anaerobic CH_4 oxidation was always a minor fraction of the potential net CH_4 production (Table 2). As suggested by the lower C:N ratio (Table 1), the vegetated littoral site had a higher availability of labile OM than the profundal site. This explained the higher potential CH_4 and TIC production,

as well as the higher relative abundance of methanogens, at the littoral site. Furthermore, the higher and lower relative abundance of *Methanobacteriaceae* and *Methanoregulaceae*, respectively, at the littoral site was most likely due to differences in the adaptation of these two major H_2+CO_2-consuming freshwater methanogenic groups to variations in the substrate supply (Borrel *et al*. 2011). Together with the acetate-consuming *Methanosaetaceae*, these families were also the dominant methanogens in the investigated lakes, which agrees with the results obtained from many freshwater lakes (Borrel *et al*. 2011). The generally lower abundance and activity of the H_2+methyl-compound-consuming methanogens also agrees with previous results obtained from lakes and ponds (Crevecoeur, Warwick and Lovejoy 2016; Fan and Xing 2016). Yet, to the best of our knowledge, this is the first report showing active *mcrA* expression (albeit low) by the very recently described phyla *Verstraetearchaeota* (Vanwonterghem *et al*. 2016) in any environment, as well as the second report after a study from Lake Pavin (Biderre-Petit *et al*. 2011), to show the active *mcrA* expression of *Methanomassiliicoccales* in lake sediments.

One possible mechanism behind the EA-induced decrease in methanogenesis is the direct inhibition of methanogens, as has been shown with NO_3^- (Klüber and Conrad 1998) and Fe^{3+} (van Bodegom, Scholten and Stams 2004), which could be expected to also take place with Mn^{4+} (either directly or via the Mn^{4+}-driven oxidation of Fe^{2+} to Fe^{3+}). However, the increased availability of NO_3^- did not inhibit CH_4 production in the two deepest layers at the profundal site ($P_{90–130}$ and $P_{490–310}$), as would have been expected, if it had directly inhibited the methanogens. In addition, neither the relative abundance, nor the *mcrA* expression of the H_2+CO_2-consuming methanogens were affected by Fe^{3+} or Mn^{4+}, as would have been expected, given that they are more sensitive than acetate-consuming methanogens to the inhibitory effects of Fe^{3+} (van Bodegom, Scholten and Stams 2004). Yet, the Fe^{3+}- and Mn^{4+}-induced changes in the abundance

and activity of some individual methanogenic OTUs indicated that the slight inhibition of H_2+CO_2-consuming methanogens may have taken place, although it could not have been predominantly responsible for such large reductions in the potential net CH_4 production. The *mcrA* expression data also suggest that the H_2+methyl-compound-consuming methanogens were slightly inhibited by Fe^{3+}. However, due to their low abundance, the inhibition of their activity could not have resulted in the observed decreases in CH_4 production. Thus, the inhibition of methanogens was not an important factor underlying the decrease in the potential net CH_4 production.

The EA-induced decrease in CH_4 production was much more likely due to outcompetition of the methanogens for methanogenic substrates by anaerobically respiring bacteria (Klüpfel *et al*. 2014). The larger Fe^{3+}- and Mn^{4+}-induced changes seen in the bacterial communities rather than in the archaeal communities also support this view. The reduction of Mn^{4+}, Fe^{3+}, and NO_3^- could also produce SO_4^{2-}, S^0 (e.g. the cryptic sulfur cycle; Holmkvist, Ferdelman and Jørgensen 2011; Pester *et al.* 2012) and organic EAs (Lovley *et al.* 1996; Kappler *et al.* 2004), while that of Mn^{4+} and NO_3^- could produce Fe^{3+} (Canfield, Kristensen and Thamdrup 2005). Therefore, at least part of the Fe^{3+}-, Mn^{4+}-, and NO_3^--induced decrease in CH_4 production could also be due to anaerobic respiration coupled with EAs with a lower reduction potential. The negligible effect of NO_3^- and SO_4^{2-} on the potential net CH_4 production in the two deepest layers ($P_{90–130}$ and $P_{390–410}$) of the profundal zone (Table 2) is probably due to the relatively low number of competing anaerobically respiring bacteria. Unfortunately, molecular data were not collected from these layers. It can, however, be speculated that the populations of anaerobically respiring bacteria in the deep layers is low due to the lack of EAs. As EAs are already very efficiently consumed in the surface sediments, the two deepest layers of the

profundal zone have not been exposed to oxidized forms of nitrogen and sulfur for at least 1000 years.

As hypothesized, both Fe^{3+} and Mn^{4+} decreased the potential net production rates of CH_4 and TIC in $P_{0–10}$. This strongly suggests that besides increasing anaerobic respiration, Fe^{3+} and Mn^{4+} also induced decreases in methanogenesis via increasing OM recalcitrance and protecting it from microbial degradation (Lalonde *et al*. 2012; Karvinen, Lehtinen and Kankaala 2015; Estes *et al*. 2017). The effects of Mn^{4+} could have also been partially caused by Fe^{3+} produced via the Mn^{4+}-induced oxidation of the indigenous Fe^{2+} (Canfield, Kristensen and Thamdrup 2005). Furthermore, the decreased heterotrophic respiration processes might have led to an increase in the rate of the CO_2-fixing chemolithoautotrophic processes (via competitive release), which further contributed to the reduction in the potential net TIC production. Indeed, the uncoupling of a large part of the Fe^{3+} and Mn^{4+} reduction from the TIC production in the Fe^{3+}- and Mn^{4+}-amended treatments indicates that a significant chemolithoautotrophic and abiotic Fe^{3+} and Mn^{4+} reduction took place. The susceptibility of the sediment OM to the effects of Fe^{3+} and Mn^{4+} probably depends on the sediment type, as indicated by the lack of a Fe^{3+}- and Mn^{4+}-induced decrease in the potential net TIC production in $P_{10–30}$ (Table 2). As highly labile OM fractions (proteins and carbohydrates) were suggested to preferentially bind to iron in the sediments (Lalonde *et al*. 2012), the difference between the study layers was probably due to the higher lability of OM (as indicated by the lower C:N ratio; Table 1) in $P_{0–10}$.

In accordance with the differences in the effects of increased Fe^{3+} and Mn^{4+} on CH_4 and TIC production, the responses of the bacterial communities also differed between the study layers ($P_{0\text{-}10}$ and $P_{10\text{-}30}$) at the profundal site. There are several mechanisms which could explain this and thus are briefly discussed here. The lack of a Fe^{3+}- and Mn^{4+}-induced increase in the

relative abundance of the most typical metal-reducing sediment bacterial genus in $P_{0–10}$, *Geobacter* (Coates *et al*. 1996; Lovley 2006), could be due to the decreased OM availability in that layer. OTUs belonging to *Chloroflexi*, *Betaproteobacteria*, and *Elusimicrobia* were probably more competitive than *Geobacter* in low OM conditions. Most known species of *Chloroflexi* (e.g. Yamada and Sekiguchi 2009) and *Elusimicrobia* (e.g. Herlemann *et al*. 2009) are fermentative. Therefore, besides being more competitive than *Geobacter* in low OM conditions, their increase implies that they were fermenting and hence gained an advantage over the other fermenters by using Fe^{3+} and Mn^{4+} as minor electron sinks (Lovley 2006). However, the metabolic capabilities of many phyla are not sufficiently understood. For example, *Chloroflexi* may also harbor species capable of Fe^{3+} respiration (Kawaichi *et al*. 2013), while the Fe^{3+} respiration capability is dispersed into at least three orders within *Betaproteobacteria* (Pronk *et al*. 1992; Cummings *et al*. 1999; Finneran, Johnsen and Lovley 2003). Thus, it is possible that OTUs showing a Fe^{3+}- or Mn^{4+}-induced increase in their relative abundance in $P_{0–10}$ were also using Fe^{3+} or Mn^{4+} as EAs in anaerobic respiration.

However, as discussed above, the suppression of heterotrophic processes could have led to an increase in Fe^{3+}- and Mn^{4+}-reducing chemolithoautotrophic processes in $P_{0–10}$. Consequently, differences in the responses of the bacterial communities between the investigated layers may partially reflect the higher contribution of chemolithoautotrophic organisms in $P_{0–10}$. Furthermore, both chemolithoautotrophic and abiotic Fe^{3+} and Mn^{4+} reduction can increase the availability of SO_4^{2-}, S^0, and organic EAs (Lovley *et al*. 1996; Kappler *et al*. 2004; Canfield, Kristensen and Thamdrup 2005; Pester *et al*. 2012). Therefore, the differences in the Fe^{3+}- and Mn^{4+}-induced responses of the bacterial communities between the study layers could also be partially due to the larger contribution of anaerobically respiring bacteria capable of reducing

SO_4^{2-}, S^0, and organic EA in $P_{0–10}$. Only one OTU related to a taxon that contains species capable of SO_4^{2-} reduction and S^0 disproportionation (*Desulfobulbaceae*; Finster 2008) was slightly affected by Mn^{4+} in $P_{0–10}$. However, many freshwater SO_4^{2-} reducers belong to unknown phylogenetic lineages (Pester *et al*. 2012). Furthermore, besides the known Fe^{3+}-reducing bacteria (Lovley 2006), the bacteria that utilize organic EAs are mostly unknown. In fact, a large fraction of the bacteria that reduced organic EAs (e.g. humic acids) could not use Fe^{3+} in a previously studied lake sediment (Kappler *et al.* 2004). Further studies are therefore needed to assess the role of each discussed mechanism in explaining the bacterial community variations induced by the increased $Fe^{3+}$and Mn^{4+}. These studies could use, for example, $^{13}CO_2$ labelling to reveal the role of chemolithoautotrophy (^{13}C transfer to bulk biomass) and the active chemolithoautotrophic organisms (stable isotope probing of DNA and RNA). The studies could also individually test the effects of the addition of each inorganic EA (Fe^{3+}, Mn^{4+}, SO_4^{2-}, and S^0) and some organic EA compounds (e.g. humic acids; anthraquinone-2, -6, disulfonate) on the microbial community structure, as well as on the potential (metagenomics) and actively expressed (metatranscriptomics) metabolic pathways, for example, the pathways of fermentation and anaerobic respiration.

CONCLUSION

This study tested the effects of increased Fe^{3+} and Mn^{4+} availability on the structure of microbial communities, as well as the effects of increased Fe^{3+}, Mn^{4+}, NO_3^-, and SO_4^{2-} on the potential CH_4 oxidation and net production rates of CH_4 and TIC in boreal lake sediments for the first time. The results suggest that anaerobic CH_4 oxidation (via AOM or TMO) was not an important factor in reducing CH_4 emissions from the sediments of the two shallow study lakes. The results

further suggest that the regeneration of the sediment EA pool during oxidation events via water-column mixing, as well as via biological and physical turbation, may suppress CH_4 emissions from the lake sediments by decreasing methanogenesis and increasing MO, but not by increasing AOM. Comparing our results with those of previous lake sediment AOM studies also suggests that the abundance and activity of AOM microbes might decrease with the decreasing environmental stability associated with decreasing water column depth. In addition to the outcompetition of methanogens for methanogenic substrates by anaerobically respiring bacteria, this study suggests that increased protection of OM from microbial degradation (i.e. increased OM recalcitrance by Fe^{3+} and Mn^{4+}) is also a very important component of the Fe^{3+}- and Mn^{4+}-induced reduction in methanogenesis in lake sediments. Yet, the magnitude and controlling factors (e.g. sediment OM quality as well as Fe and Mn content) of these two mechanisms, which decrease methanogenesis, remain unclear. In order to better constrain both global and regional CH_4 budgets, it is especially important to determine whether AOM has any ecological relevance as well as to find out the importance and controlling factors of the different methanogenesis-decreasing mechanisms in the numerous small and shallow lakes and ponds in boreal and tundra landscapes, which represent globally significant sources of CH_4 to the atmosphere (Wik *et al.* 2016). Future studies should also specifically address the role of organic EAs in affecting methane production and consumption in lake sediments.

This study offers new insights into the mechanisms preserving OM in boreal lake sediments. They are effective C sinks due to the low temperature and recalcitrant nature of OM, which serve to constrain the microbial metabolism (Kortelainen *et al*. 2004; Gudasz *et al*. 2012). As noted here and in previous studies (Lalonde *et al*. 2012; Estes *et al*. 2017), the reactions of OM with Fe^{3+} and Mn^{4+} further increase OM preservation. However, the observed increase in C

degradation (TIC production), which was solely driven by the addition of O_2 (and not by the addition of any other EA) in the study sediments, also explains why anoxia plays an important role in retaining C in boreal lake sediments. This suggests that O_2-consuming microbial processes are crucial in inducing sediment C storage. Besides generating anoxia, they increase OM recalcitrance via consuming labile OM and via oxidizing Fe^{2+} and Mn^{2+} to Fe^{3+} and Mn^{4+}, which react with OM (Lalonde *et al*. 2012; Estes *et al*. 2017). Whether or not the Fe^{3+}- and Mn^{4+}-induced inhibition of heterotrophic OM degradation processes could also benefit the chemolithoautotrophic processes that additionally increase sediment C storage via CO_2 fixation requires further study.

FUNDING

This work was supported by The Academy of Finland [136455 and 140964 to HN, 286642 to AJR, and 260797 to MT] and Maj & Tor Nessling foundation [AK and PK].

ACKNOWLEDGEMENTS

We thank S. Hietanen and B. Thamdrup for helpful comments on this manuscript and K. Ratilainen for his help with collecting sediment samples. We also thank the two anonymous reviewers and the editor for their constructive comments.

Conflict of interest. None declared.

REFERENCES

Altschul SF, Gish W, Miller W *et al*. Basic local alignment search tool. *J Mol Biol* 1990;**215**:403-410.

Anderson MJ. A new method for non-parametric multi-variate analysis of variance. *Austral Ecol* 2001;**26**:32-46.

Bastviken D, Cole J, Pace M *et al*. Methane emissions from lakes: dependence of lake characteristics, two regional assessments, and a global estimate. *Global Biogeochem Cy* 2004;**18**:GB4009.

Beal EJ, House CH, Orphan VJ. Manganese- and iron-dependent marine methane oxidation. *Science* 2009;**325**:184-187.

Bedard C, Knowles R. Hypolimnetic O_2 consumption, denitrification, and methanogenesis in a thermally stratified lake. *Can J Fish Aquat Sci* 1991;**48**:1048–1054.

Biderre-Petit C, Jézéquel D, Dugat-Bony E. *et al*. Identification of microbial communities involved in the methane cycle of a freshwater meromictic lake. *FEMS Microbiol Ecol* 2011;**77**:533-545.

Blazewicz SJ, Petersen DG, Waldrop MP *et al*. Anaerobic oxidation of methane in tropical and boreal soils: ecological significance in terrestrial methane cycling. *J Geophys Res* 2012; **117**:G02033.

Blees J, Niemann H, Wenk CB *et al*. Micro-aerobic bacterial methane oxidation in the chemocline and anoxic water column of deep south-Alpine Lake Lugano (Switzerland). *Limnol Oceanogr* 2014;**59**:311-324

Borrel G, Jézéquel D, Biderre-Petit C *et al*. Production and consumption of methane in freshwater lake ecosystems. *Res Microbiol* 2011;**162**:832-847.

Borrel G, Lehours A-C, Crouzet O *et al*. Stratification of archaea in the deep sediments of a freshwater meromictic lake: vertical shift from methanogenic to uncultured archaeal lineages. *PLoS One* 2012;**7**:e43346.

Borrel G, O´Toole PW, Harris HMB *et al*. Phylogenomic data support a seventh order of methylotrophic methanogens and provide insights into the evolution of methanogenesis. *Genom Biol Evol* 2013;**5**:1769-1780.

Bretz KA, Whalen SC. Methane cycling dynamics in sediments of Alaskan Arctic Foothill lakes. *Inland Waters* 2014;**4**:65-78.

Canfield DE, Kristensen E, Thamdrup B. *Aquatic Geomicrobiology*. San Diego: Elsevier Academic Press, 2005.

Chan OC, Claus P, Casper P *et al*. Vertical distribution of structure and function of the methanogenic archaeal community in Lake Dagow sediment. *Environ Microbiol* 2005;**7**:1139-1149.

Chowdhury TR, Dick RP. Ecology of aerobic methanotrophs in controlling methane fluxes from wetlands. *Appl Soil Ecol* 2013;**65**:8-22.

Coates JD, Phillips EJP, Lonergan DJ *et al*. Isolation of *Geobacter* species from diverse sedimentary environments. *Appl Environ Microbiol* 1996;**62**:1531-1536.

Conrad R. Contribution of hydrogen to methane production and control of hydrogen concentrations in methanogenic soils and sediments. *FEMS Microbiol Ecol* 1999;**28**:193-202.

Conrad R, Chan OC, Claus P *et al*. Characterization of methanogenic Archaea and stable isotope fractionation during methane production in the profundal sediment of an oligotrophic lake (Lake Stechlin, Germany). *Limnol Oceanogr* 2007;**52**:1393-1406.

Conrad R, Klose M, Claus P *et al*. Methanogenic pathway, ^{13}C isotope fractionation, and archaeal community composition in the sediment of two clear-water lakes of Amazonia. *Limnol Oceanogr* 2010;**55**:689-702.

Crevecoeur S, Warwick VF, Lovejoy C. Environmental selection of planktonic methanogens in permafrost thaw ponds. *Sci Rep* 2016;**6**:31312.

Cummings DE, Caccavo Jr F, Spring S *et al*. *Ferribacterium limneticum*, gen. nov., sp. nov., an Fe(III)-reducing microorganism isolated from mining-impacted freshwater lake sediments. *Arch Microbiol* 1999;**171**:183-188.

Deutzmann JS, Stief P, Brandes J *et al*. Anaerobic methane oxidation coupled to denitrification is the dominant methane sink in a deep lake. *PNAS* 2014;**111**:18273-18278.

Ding J, Fu L, Ding Z-W *et al.* Experimental evaluation of the metabolic reversibility of ANME-2d between anaerobic methane oxidation and methanogenesis. *Appl Microbiol Biotechnol* 2016;**100**:6481-6490.

Edgar RC, Haas BJ, Clemente JC *et al.* UCHIME improves sensitivity and speed of chimera detection. *Bioinformatics* 2011;**27**:2194-2200.

Estes ER, Andeer PF, Nordlund D *et al*. Biogenic manganese oxides as reservoirs of organic carbon and proteins in terrestrial and marine environments. *Geobiology* 2017;**15**:158-172.

Ettwig KF, Butler MK, Le Paslier D *et al*. Nitrite-driven anaerobic methane oxidation by oxygenic bacteria. *Nature* 2010;**464**:543-548.

Ettwig KF, van Alen T, van de Pas-Schoonen KT *et al*. Enrichment and molecular detection of denitrifying methanotrophic bacteria of the *NC10* phylum. *Appl Environ Microbiol* 2009;**75**:3656-3662.

Ettwig KF, Zhu B, Speth D *et al*. Archaea catalyze iron-dependent anaerobic oxidation of methane. *PNAS* 2016;**113**:12792-12796.

Evans PN, Parks DH, Chadwick GL *et al.* Methane metabolism in the archaeal phylum *Bathyarchaeota* revealed by genome-centric metagenomics. *Science* 2015;**350**:434-438.

Fan X, Xing P. Differences in the composition of archaeal communities in sediments from contrasting zones of Lake Taihu. *Front Microbiol* 2016;**7**:1510.

Finneran KT, Johnsen CV, Lovley DR. *Rhodoferax ferrireducens* sp. nov., a psychrotolerant, facultatively anaerobic bacterium that oxidizes acetate with the reduction of Fe(III). *Int J Syst Evol Microbiol* 2003;**53**:669-673.

Finster K. Microbiological disproportionation of inorganic sulfur compounds. *J Sulfur Chem* 2008;**29**:281-292.

Gantner S, Andersson AF, Alonso-Sáez L *et al*. Novel primers for 16S rRNA based archaeal community analyses in environmental samples. *J Microbiol Meth* 2011;**84**:12-18.

Griffiths RI, Whiteley AS, O'Donnell AG *et al.* Rapid method for coextraction of DNA and RNA from natural environments for analysis of ribosomal DNA- and rRNA-based microbial community composition. *Appl Environ Microbiol* 2000;**66**:5488–5491.

Gudasz C, Bastviken D, Premke K *et al*. Constrained microbial processing of allochthonous organic carbon in boreal lake sediments. *Limnol Oceanogr* 2012;**57**:163-175.

Hammer Ø, Harper DAT, Ryan PD. PAST: paleontological statistics software package for education and data analysis. *Palaeontol Electron* 2001;**4**:9pp.

Hanson RS, Hanson TE. Methanotrophic bacteria. *Microbiol Rev* 1996;**60**:439-471.

Haroon MF, Hu S, Shi Y *et al*. Anaerobic oxidation of methane coupled to nitrate reduction in a novel archaeal lineage. *Nature* 2013;**500**:567-570.

Herlemann DPR, Geissinger O, Ikeda-Ohtsubo W *et al*. Genomic analysis of "*Elusimicrobium minutum*," the first cultivated representative of the phylum "*Elusimicrobia*" (Formerly Termite Group 1). *Appl Environ Microbiol* 2009;**75**:2841-2849.

Hiscock K, Bense V. *Hydrogeology: Principles and Practice*. John Wiley & Sons, 2014.

Holmer M, Storkholm P. Sulphate reduction and sulphur cycling in lake sediments: a review. *Freshwater Biology* 2001;**46**:431-451.

Holmkvist L, Ferdelman TG, Jørgensen BB. A cryptic sulfur cycle driven by iron in the methane zone of marine sediment (Aarhus Bay, Denmark). *Geochim Cosmochim Acta* 2011;**75**:3581-3599.

Huerta-Diaz MA, Tessier A, Carignan R. Geochemistry of trace metals associated with reduced sulfur in freshwater sediments. *Applied Geochemistry* 1998;**13**:213-233.

Huse SM, Welch DM, Morrison HG *et al.* Ironing out the wrinkles in the rare biosphere through improved OTU clustering. *Environ Microbiol* 2010;**12**:1889–1898.

Juutinen S, Alm J, Larmola T *et al*. Major implication of the littoral zone for methane release from boreal lakes. *Global Biogeochem Cy* 2003;**17**:1117.

Kallistova AY, Goel G, Nozhevnigova AN. Microbial diversity of methanogenic communities in the systems for anaerobic treatment of organic waste. *Microbiology* 2014;**83**:462-483.

Kankaala P, Taipale S, Nykänen H *et al*. Oxidation, efflux, and isotopic fractionation of methane during autumnal turnover in a polyhumic, boreal lake. *J Geophys Res* 2007;**112**:G02033.

Kappler A, Benz M, Schink B *et al*. Electron shuttling via humic acids in microbial iron(III) reduction in a freshwater sediment. *FEMS Microbiol Ecol* 2004;**47**:85-92.

Karvinen A, Lehtinen L, Kankaala P. Variable effects of iron (Fe (III)) additions on potential methane production in boreal lake littoral sediments. *Wetlands* 2015;**35**:137-146.

Kawaichi S, Ito N, Kamikawa R *et al. Ardenticatena maritima* gen. nov., sp. nov., a ferric iron- and nitrate-reducing bacterium of the phylum '*Chloroflexi*' isolated from an iron-rich coastal hydrothermal field, and description of *Ardenticatenia* classis nov. *Int J Syst Evol Microbiol* 2013;**63**:2992-3002.

Klüber HD, Conrad R. Effects of nitrate, nitrite, NO and N_2O on methanogenesis and other redox processes in anoxic rice field soil. *FEMS Microbiol Ecol* 1998;**25**:301-318.

Klüpfel L, Piepenbrock A, Kappler A *et al*. Humic substances as fully regenerable electron acceptors in recurrently anoxic environments. *Nature Geosci* 2014;**7**:195-200.

Knittel K, Boetius A. Anaerobic oxidation of methane: progress with an unknown process. *Annu Rev Microbiol* 2009;**63**:311-334.

Kojima H, Tsutsumi M, Ishikawa K *et al*. Distribution of putative denitrifying methane oxidizing bacteria in a sediment of a freshwater lake, Lake Biwa. *Syst Appl Microbiol* 2012;**35**:233-238.

Kortelainen P, Pajunen H, Rantakari M *et al*. A large carbon pool and small sink in boreal Holocene lake sediments. *Glob Change Biol* 2004;**10**:1648-1653.

Lalonde K, Mucci A, Ouellet A *et al*. Preservation of organic matter in sediments promoted by iron. *Nature* 2012;**483**:198–200.

Lazar CS, Biddle JF, Meador TB *et al*. Environmental controls on intragroup diversity of the uncultured benthic *archaea* of the miscellaneous Crenarchaeotal group lineage naturally enriched in anoxic sediments of the White Oak River estuary (North Carolina, USA). *Environ Microbiol* 2015;**17**:2228-2238.

Lovley D. Dissimilatory Fe(III)- and Mn(IV)-reducing prokaryotes. *Prokaryotes* 2006;**2**:635-658.

Lovley DR, Coates JD, Blunt-Harris EL *et al*. Humic substances as electron acceptors for microbial respiration. *Nature* 1996;**382**:445-448.

Lovley DR, Phillips EJP. Organic matter mineralization with reduction of ferric iron in anaerobic sediments. *Appl Environ Microbiol* 1986;**51**:683-689.

Lovley DR, Phillips EJP. Novel mode of microbial energy metabolism: organic carbon oxidation coupled to dissimilatory reduction of iron or manganese. *Appl Environ Microbiol* 1988;**54**:1472-1480.

Marotta H, Pinho L, Gudasz C *et al*. Greenhouse gas production in low-latitude lake sediments responds strongly to warming. *Nature Climate Change* 2014;**4**:467-470.

Mattson MD, Likens GE. Redox reactions of organic matter decomposition in a soft water lake. *Biogeochem* 1993;**19**:149–172.

McArdle BH, Anderson MJ. Fitting multivariate models to community data: a comment on distance-based redundancy analysis. *Ecology* 2001;**82**:290 –297.

McCune B, Mefford MJ. *PC-ORD. Multivariate analysis of ecological data*. Version 6. MjM Software, Gleneden Beach, Oregon, USA, 2011.

Meulepas RJW, Jagersma CG, Zhang Y *et al*. Trace methane oxidation and the methane dependency of sulfate reduction in anaerobic granular sludge. *FEMS Microbiol Ecol* 2010;**72**:261-271.

Miller LG, Sasson C, Oremland RS. Difluoromethane, a new and improved inhibitor of methanotrophy. *Appl Environ Microbiol* 1998;**64**:4357-4362.

Molot LA, Dillon PJ. Storage of terrestrial carbon in boreal lake sediments and evasion to the atmosphere. *Global Biogeochem Cy* 1996;**10**:483-492.

Moran JJ, House CH, Freeman KH *et al*. Trace methane oxidation studied in several Euryarchaeota under diverse conditions. *Archaea* 2005;**1**:303-309.

Moran JJ, House CH, Thomas B *et al*. Products of trace methane oxidation during nonmethylotrophic growth by *Methanosarcina*. *J Geophys Res* 2007;**112**:G02011.

Nazaries L, Murrell JC, Millard P *et al*. Methane, microbes and models: fundamental understanding of the soil methane cycle for future predictions. *Environ Microbiol* 2013;**15**:2395-2417.

á Norði K, Thamdrup B. Nitrate-dependent anaerobic methane oxidation in a freshwater sediment. *Geochim Cosmochim Ac* 2014;**132**:141-150.

á Norði K, Thamdrup B, Schubert CJ. Anaerobic oxidation of methane in an iron-rich Danish freshwater lake sediment. *Limnol Oceanogr* 2013;**58**:546-554.

Nykänen H, Peura S, Kankaala P *et al*. Recycling and fluxes of carbon gases in a stratified boreal lake following experimental carbon addition. *Biogeosci Discuss* 2014;**11**:16447–16495.

Pajunen H. *Järvisedimentit kuiva-aineen ja hiilen varastona*. Geological Survey of Finland, Report of Investigation 160, 2004. (In Finnish with English summary: Lake sediments as a store of dry matter and carbon)

Pester M, Knorr K-H, Friedrich MW *et al*. Sulfate-reducing microorganisms in wetlands – fameless actors in carbon cycling and climate change. *Front Microbiol* 2012;**3**:72.

Pronk JT, de Bruyn JC, Bos P *et al*. Anaerobic growth of *Thiobacillus ferrooxidans*. *Appl Environ Microbiol* 1992;**58**:2227-2230.

Rissanen AJ, Tiirola M, Hietanen S *et al*. Interlake variation and environmental controls of denitrification across different geographical scales. *Aquat Microb Ecol* 2013;**69**:1-16.

Salonen, K. 1981. Rapid and precise determination of total inorganic carbon and some gases in aqueous solutions. *Water Res* 1981;**15**:403-406.

Scheller S, Yu H, Chadwick GL *et al*. Artificial electron acceptors decouple archaeal methane oxidation from sulfate reduction. *Science* 2016;**351**:703-707.

Schloss PD, Gevers D, Westcott SL. Reducing the effects of PCR amplification and sequencing artifacts on 16S rRNA-based studies. *PLoS One* 2011;**6**:e27310.

Schloss PD, Westcott SL, Ryabin T *et al*. Introducing mothur: open-source, platform-independent, community-supported software for describing and comparing microbial communities. *Appl Environ Microbiol* 2009;**75**:7537-7541.

Schulz S, Matsuyama H, Conrad R. Temperature dependence of methane production from different precursors in a profundal sediment (Lake Constance). *FEMS Microbiol Ecol* 1997;**22**: 207-213.

Schubert CJ, Vazquez F, Lösekann-Behrens T et al. Evidence for anaerobic oxidation of methane in sediments of a freshwater system (Lago di Cadagno). *FEMS Microbiol Ecol* 2011;**76**:26–38.

Segarra KEA, Comerford C, Slaughter J *et al*. Impact of electron acceptor availability on the anaerobic oxidation of methane in coastal freshwater and brackish wetland sediments. *Geochim Cosmochim Acta* 2013;**115**:15-30.

Segata N, Izard J, Waldron L *et al*. Metagenomic biomarker discovery and explanation. *Genome Biol* 2011;**12**:R60.

Shen L, Wu H, Gao Z *et al*. Comparison of community structures of *Candidatus* Methylomirabilis oxyfera-like bacteria of NC10 phylum in different freshwater habitats. *Sci Rep* 2016;**6**:25647.

Sivan O, Adler M, Pearson A *et al*. Geochemical evidence for iron-mediated anaerobic oxidation of methane. *Limnol Oceanogr* 2011;**56**:1536-1544.

Stumm W, Morgan JJ. *Aquatic chemistry. An introduction emphasizing chemical equilibria in natural waters*. New York: John Wiley & Sons, 1981.

Timmers PH, Suarez-Zuluaga DA, van Rossem M *et al*. Anaerobic oxidation of methane associated with sulfate reduction in a natural freshwater gas source. *ISME J* 2016;**10**:1400-1412.

Timmers PHA, Welte CU, Koehorst JJ *et al.* Reverse methanogenesis and respiration in methanotrophic archaea. *Archaea* 2017; **2017**:article ID 1654237

Van Bodegom PM, Scholten JCM, Stams AJM. Direct inhibition of methanogenesis by ferric iron. *FEMS Microbiol Ecol* 2004;**49**:261-268.

Vanwonterghem I, Evans PN, Parks DH. *et al*. Methylotrophic methanogenesis discovered in the archaeal phylum Verstraetearchaeota. *Nat Microbiol* 2016;**1**:16170; doi:10.1038/nmicrobiol.2016.170.

Vicca S, Flessa H, Loftfield N *et al*. The inhibitory effect of difluoromethane on CH_4 oxidation in reconstructed peat columns and side-effects on CO_2 and N_2O emissions at two water levels. *Soil Biol Biochem* 2009;**41**:1117-1123.

Wang Q, Garrity GM, Tiedje JM *et al*. Naïve Bayesian classifier for rapid assignment of rRNA sequences into the new bacterial taxonomy. *Appl Environ Microbiol* 2007;**73**:5261-5267.

Wang Q, Quensen III JF, Fish JA *et al*. Ecological patterns of *nifH* genes in four terrestrial climatic zones explored with targeted metagenomics using FrameBot, a new informatics tool. *mBio* 2013;**4**:e00592-13.

Wasmund K, Schreiber L, Lloyd KG *et al*. Genome sequencing of a single cell of the widely distributed marine subsurface *Dehalococcoidia*, phylum *Chloroflexi*. *ISME J* 2014;**8**:383-397.

Welte CU, Rasigraf O, Vaksmaa A *et al*. Nitrate- and nitrite-dependent anaerobic oxidation of methane. *Environ Microbiol Rep* 2016;**8**:941-955.

Wik M, Varner RK, Anthony KW et al. Climate sensitive northern lakes and ponds are critical components of methane release. *Nature Geosci* 2016;**9**:99-105.

Wrighton KC, Castelle CJ, Wilkins MJ *et al*. Metabolic interdependencies between phylogenetically novel fermenters and respiratory organisms in an unconfined aquifer. *ISME J* 2014;**8**:1452-1463.

Yamada T, Sekiguchi Y. Cultivation of uncultured *Chloroflexi* subphyla: Significance and ecophysiology of formerly uncultured *Chloroflexi* 'Subphylum I' with natural and biotechnological relevance. *Microbes Environ* 2009;**24**:205-216.

Zheng H, Dietrich C, Radek R *et al*. *Endomicrobium proavitum*, the first isolate of *Endomicrobia* class. nov. (phylum *Elusimicrobia*) – an ultramicrobacterium with an unusual cell cycle that fixes nitrogen with a Group IV nitrogenase. *Environ Microbiol* 2016;**18**:191-204.

Table 1. Sample codes and characteristics of the study sediments. Age is estimated according to Pajunen (2004). n.d. = not determined.

Sample code	Site	Layer (cm)	Age (y)	dry matter (%)	C (%)	N (%)	C:N	[Fe] ($\mu mol\ g^{-1}_{DW}$)	[Mn] ($nmol\ g^{-1}_{DW}$)
L_{0-25}	Littoral	0-25	n.d.	19.4	4.80	0.48	10.0	130	100
P_{0-10}	Profundal	0-10	0 – 50	13.4	7.97	0.67	11.9	270	340
P_{10-30}		10-30	50 – 150	21.8	7.22	0.46	15.7	n.d.	n.d.
P_{90-130}		90-130	1700 – 2500	14.2	11.63	0.71	16.4	n.d.	n.d.
$P_{390-410}$		390-410	6800 - 7000	24.8	7.49	0.56	13.4	n.d.	n.d.

Table 2. Potential net production rates of CH_4 and TIC as well as the potential CH_4 oxidation rates in the incubations of the sediment slurry samples subjected to different treatments in 2012 and 2014. Significant differences among the treatments at each depth layer are shown on the right side of the values with a differing letter (one-way ANOVA, $p < 0.05$). The values are shown as averages ± SD, n = 3–4. See Table 1 for a definition of the sample codes.

Year	Sample code	Treatment	net CH_4 prod. (nmol $g^{-1}_{DW}d^{-1}$)		net TIC prod. (nmol $g^{-1}_{DW}d^{-1}$)		CH_4 ox. (nmol $g^{-1}_{DW}d^{-1}$)	
2012[1]								
	L_{0-25}	CH_4	40.8±6.8	a	132.4±20.2	a	0.7±0.2	a
		$CH_4+SO_4^{2-}$	13.9±6.1	b	133.5±10.7	a	0	*0*
		$CH_4+NO_3^-$	24.4±2.9	c	124.7±4.7	a	0	*0*
		CH_4+O_2	-0.8±1.0	d	253.8±65.5	b	4.1±2.7	b
	P_{10-30}	CH_4	4.1±1.5	a	38.2±10.9	a	0	*0*
		$CH_4+SO_4^{2-}$	1.6±0.3	b	44.5±4.4	a	0	*0*
		$CH_4+NO_3^-$	1.8±0.3	b	37.4±4.2	a	0	*0*
		CH_4+O_2	-1.5±0.2	c	44.6±8.1	a	1.2±1.2	a
	P_{90-130}	CH_4	5.5±1.4	a	54.1±3.8	a	0	*0*
		$CH_4+SO_4^{2-}$	4.1±1.1	a	67.4±12.5	a	0	*0*
		$CH_4+NO_3^-$	4.7±1.1	a	51.4±11.3	a	0	*0*
		CH_4+O_2	-5.0±0.9	b	199.3±39.3	b	1.7±0.1	a
	$P_{390-410}$	CH_4	0.9±0.04	a	27.7±3.4	a	0	*0*
		$CH_4+SO_4^{2-}$	0.9±0.3	a	19.7±7.2	a	0	*0*
		$CH_4+NO_3^-$	0.6±0.4	a	25.0±8.9	a	0	*0*
		CH_4+O_2	0	*0*	98.2±27.4	b	0	*0*
2014[1]								
	P_{0-10}	CH_4	82.5±15.4	a	294.9±44.3	a	0.9±0.2	a
		CH_4+Fe^{3+}	58.1±6.6	b	118.7±9.1	b	0.6±0.2	a
		CH_4+Mn^{4+}	20.9±8.4	c	172.5±62.5	b	2.1±1.9	a
		CH_4+O_2	-72.7±3.7	d	782.4±96.1	c	49.3±16.9	b
		$CH_4+CH_2F_2$	82.3±16.5	a	318.7±60.0	a	0.6±0.1	a
	P_{10-30}	CH_4	80.1±13.9	a	120.5±5.2	a	0.2±0.1	a
		CH_4+Fe^{3+}	67.2±24.5	a	125.2±9.1	a	0.1±0.05	a
		CH_4+Mn^{4+}	13.8±5.6	b	140.8±10.4	a	0.1±0.1	a
		CH_4+O_2	-18.3±3.5	c	274.6±47.1	b	18.0±14.5	b
		$CH_4+CH_2F_2$	72.1±12.1	a	130.3±9.0	a	0.2±0.1	a

1) Incubations were done at +4°C for up to 14 months in 2012 and at +10°C for up to 4 months in 2014

Table 3. Potential Fe^{3+} reduction rate (denoted as Fe^{2+} production rate) in the incubations of the sediment slurry samples amended with or without Fe^{3+}, as well as the potential Mn^{4+} reduction rate (denoted as Mn^{2+} production rate) in the incubations of the sediment slurry samples amended with or without Mn^{4+} in 2012. Significant differences among the treatments at each depth layers are shown on the right side of the values with a differing letter (t-test, $p < 0.05$). The values are shown as averages ± SD, n = 3. n.d. = not determined. See Table 1 for a definition of the sample codes.

Sample code[1]		Fe^{2+} production (nmol $g^{-1}_{DW}d^{-1}$)		Mn^{2+} production (nmol $g^{-1}_{DW}d^{-1}$)	
L_{0-25}	no addit.	16.1±8.7	a	13.5±0.2	a
	Fe^{3+}	827.0±101.6	b	n.d	
	Mn^{4+}	n.d		1066.4±231.3	b
P_{0-10}	no addit.	748.4±66.8	a	20.8±3.8	a
	Fe^{3+}	913.3±76.0	b	n.d	
	Mn^{4+}	n.d		1009.7±113.1	b

1) Incubations were done at +10°C for up to 4.5 months

Figure legends:

Figure 1. Relative abundances (average +/- SD) of the taxonomic groups of (A) methanogenic/methanotrophic archaea based on 16S rRNA sequencing and (B) methanogenic/methanotrophic archaea (DNA) and active methanogenic/methanotrophic archaea (mRNA) based on *mcrA* gene and *mcrA* mRNA transcript sequencing before (non-incubated) and after incubations with either CH_4, CH_4+Fe^{3+} or CH_4+Mn^{4+} amendments. $L_{0\text{-}25}$, $P_{0\text{-}10}$ and $P_{10\text{-}30}$ denote 0 – 25 cm layer of the littoral and 0 – 10 cm and 10 – 30 cm layers of the profundal study site, respectively. The substrates for methanogenesis as well as the potential AOM function are shown in brackets after the taxonomic information.

Figure 2. Relative abundances (average +/- SD) of the taxonomic groups of bacteria divided into (A) fermentative bacteria, (B) Fe^{3+}/Mn^{4+} (metal) reducing bacteria, and (C) aerobic (MOB) and anaerobic (AOM) methanotrophic bacteria before (non-incubated) and after incubations with either CH_4, CH_4+Fe^{3+} or CH_4+Mn^{4+} amendments. $L_{0\text{-}25}$, $P_{0\text{-}10}$ and $P_{10\text{-}30}$ denote 0 – 25 cm layer of the littoral and 0 – 10 cm and 10 – 30 cm layers of the profundal study site, respectively.

Figure 3. Relative activity (average +/- SD) and taxonomic affiliations (and methanogenic substrate) of the *mcrA* OTUs (based on the mRNA transcripts) that differed in their relative activity among the CH_4, CH_4+Fe^{3+}, or CH_4+ Mn^{4+} treatments after the incubation of sediment slurry samples from $P_{0\text{-}10}$ (linear discriminant analysis [LDA] effect size [LEfSe] method $p < 0.05$). The OTUs are grouped into three subfigures according to the treatment in which they exhibited the highest relative abundance in comparison to the other treatments: (A) CH_4, (B) CH_4+Fe^{3+}, or (C) CH_4+Mn^{4+}.

Figure 4. Relative abundance (average +/- SD) and taxonomic affiliations of the bacterial 16S rRNA gene OTUs that differed in their relative abundance among the CH_4, CH_4+Fe^{3+}, or CH_4+Mn^{4+} treatments after the incubation of sediment slurry samples from $P_{0\text{-}10}$ (A–C) and $P_{10–30}$ (D–F) (linear discriminant analysis [LDA] effect size [LEfSe] method $p < 0.05$). The OTUs are grouped into three rows according to the treatment (CH_4, CH_4+Fe^{3+}, or CH_4+Mn^{4+}) in which they exhibited the highest relative abundance in comparison to the other treatments: (A)/(D) CH_4, (B)/(E) CH_4+Fe^{3+}, or (C)/(F) CH_4+Mn^{4+}.

Fig. 1.

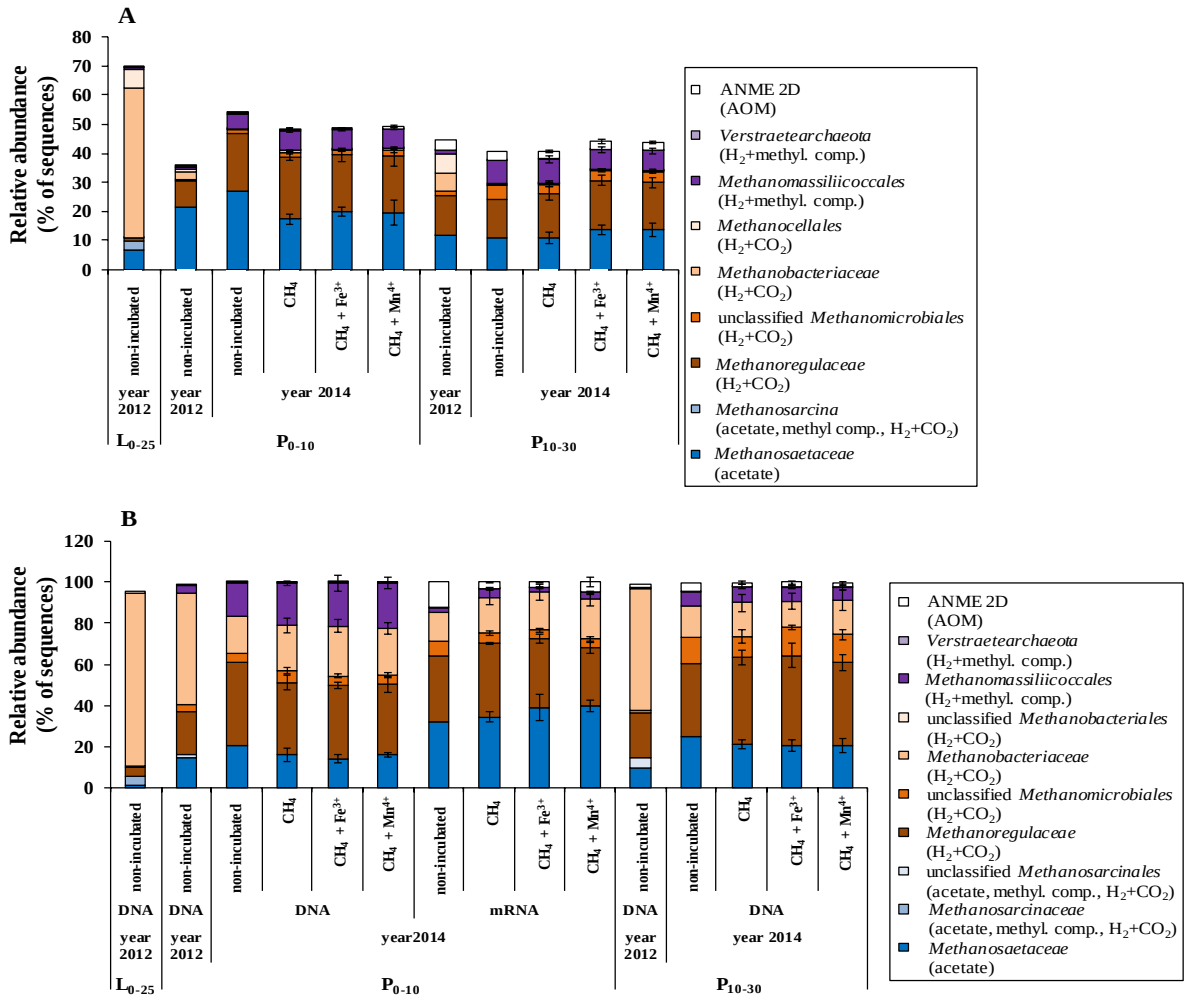
A
Relative abundance (% of sequences)
80
70
60
50
40
30
20
10
0
non-incubated
year 2012
CH4
CH4 + Fe3+
CH4 + Mn4+
year 2014
L0-25
P0-10
P10-30
ANME 2D (AOM)
Verstraetearchaeota (H2+methyl. comp.)
Methanomassiliicoccales (H2+methyl. comp.)
Methanocellales (H2+CO2)
Methanobacteriaceae (H2+CO2)
unclassified Methanomicrobiales (H2+CO2)
Methanoregulaceae (H2+CO2)
Methanosarcina (acetate, methyl comp., H2+CO2)
Methanosaetaceae (acetate)
B
Relative abundance (% of sequences)
120
100
80
60
40
20
0
DNA
mRNA
year2014
unclassified Methanobacteriales (H2+CO2)
unclassified Methanosarcinales (acetate, methyl. comp., H2+CO2)
Methanosarcinaceae (acetate, methyl. comp., H2+CO2)

Fig. 2.

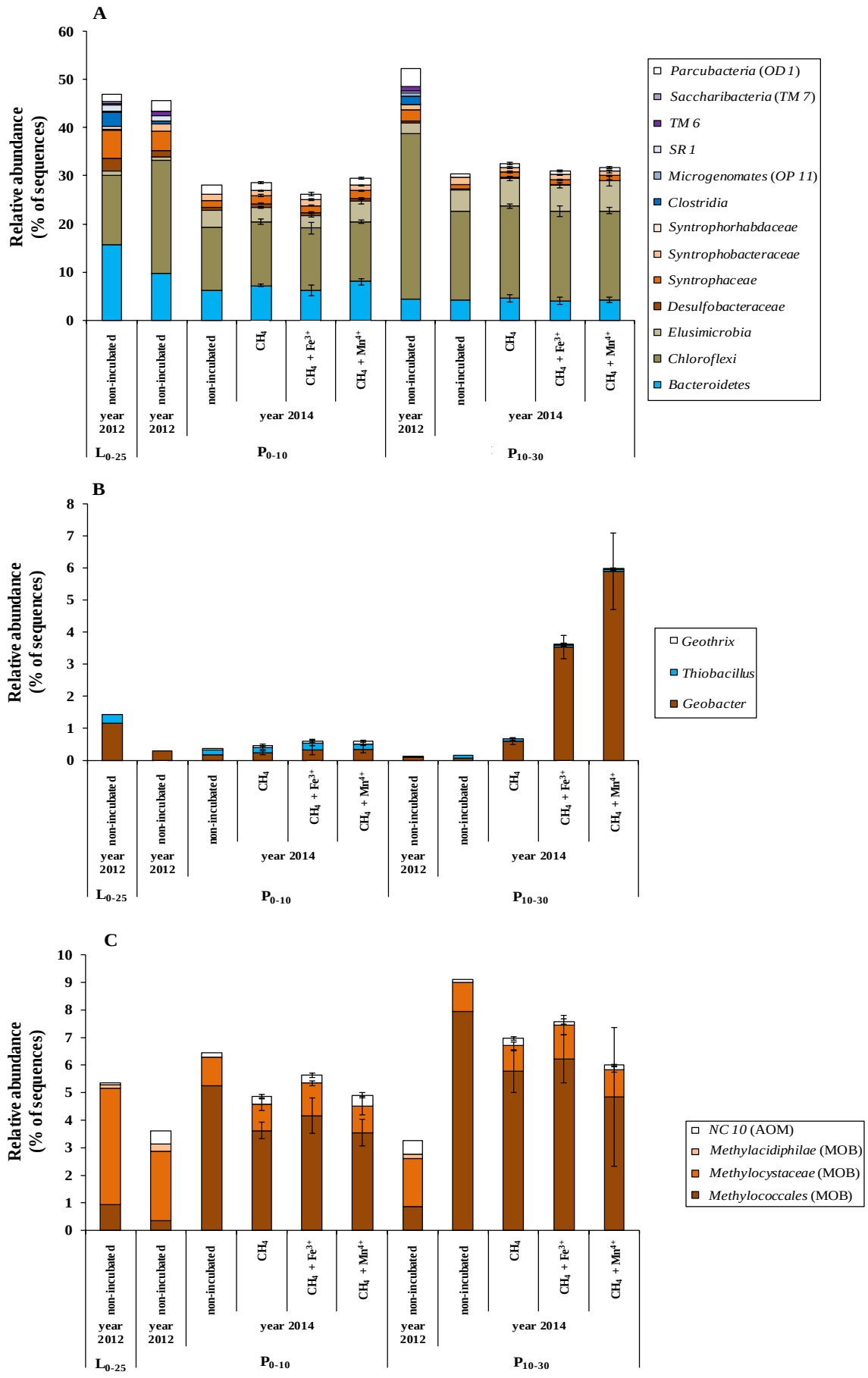
A
Relative abundance (% of sequences)
60
50
40
30
20
10
0
Parcubacteria (OD1)
Saccharibacteria (TM7)
TM6
SR1
Microgenomates (OP11)
Clostridia
Syntrophorhabdaceae
Syntrophobacteraceae
Syntrophaceae
Desulfobacteraceae
Elusimicrobia
Chloroflexi
Bacteroidetes
non-incubated
year 2012
year 2014
CH4
CH4 + Fe3+
CH4 + Mn4+
L0-25
P0-10
P10-30
B
Relative abundance (% of sequences)
8
7
6
5
4
3
2
1
0
Geothrix
Thiobacillus
Geobacter
C
Relative abundance (% of sequences)
10
9
8
7
6
5
4
3
2
1
0
NC10 (AOM)
Methylacidiphilae (MOB)
Methylocystaceae (MOB)
Methylococcales (MOB)

Fig. 3.

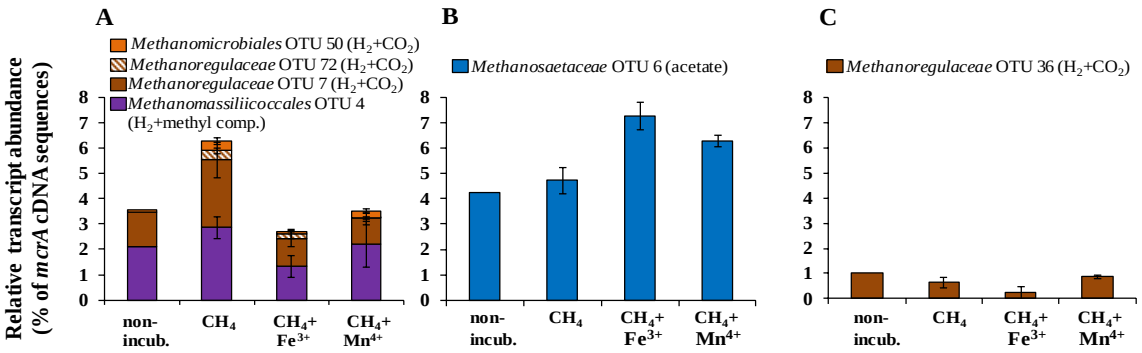
A
B
C
Relative transcript abundance (% of mcrA cDNA sequences)
Methanomicrobiales OTU 50 (H2+CO2)
Methanoregulaceae OTU 72 (H2+CO2)
Methanoregulaceae OTU 7 (H2+CO2)
Methanomassiliicoccales OTU 4 (H2+methyl comp.)
Methanosaetaceae OTU 6 (acetate)
Methanoregulaceae OTU 36 (H2+CO2)
0
1
2
3
4
5
6
7
8
non-incub.
CH4
CH4+ Fe3+
CH4+ Mn4+

Fig. 4.

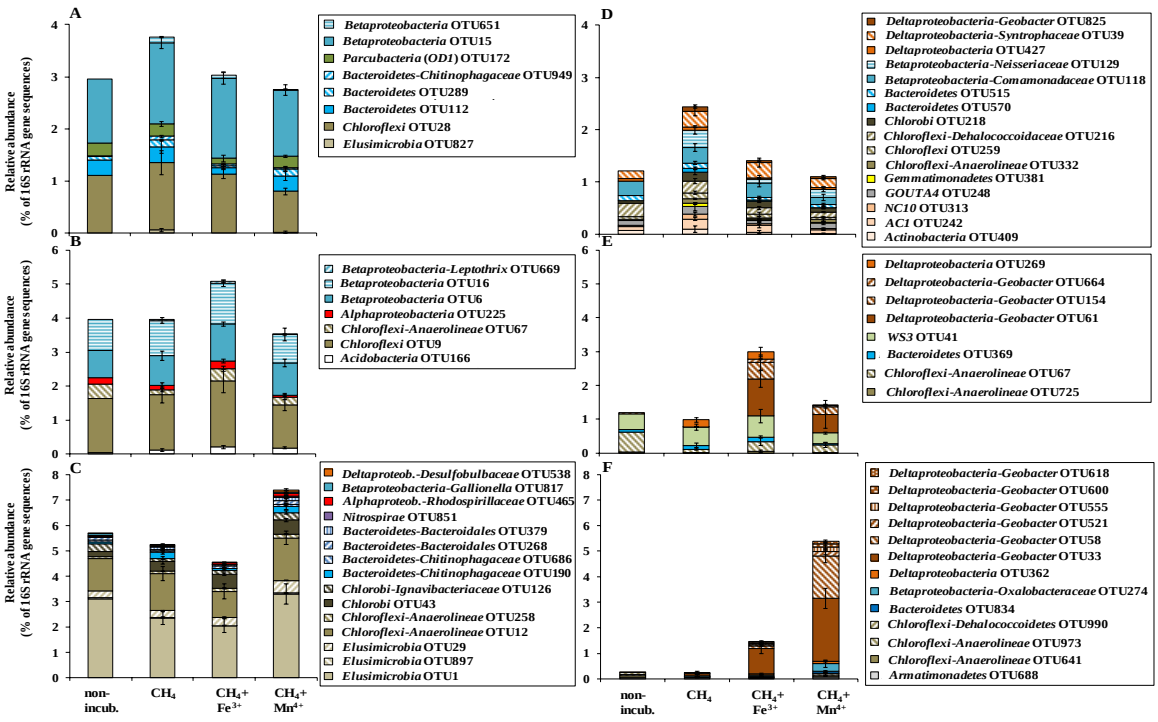
A
B
C
D
E
F
Relative abundance (% of 16S rRNA gene sequences)
Betaproteobacteria OTU651
Betaproteobacteria OTU15
Parcubacteria (OD1) OTU172
Bacteroidetes-Chitinophagaceae OTU949
Bacteroidetes OTU289
Bacteroidetes OTU112
Chloroflexi OTU28
Elusimicrobia OTU827
Betaproteobacteria-Leptothrix OTU669
Betaproteobacteria OTU16
Betaproteobacteria OTU6
Alphaproteobacteria OTU225
Chloroflexi-Anaerolineae OTU67
Chloroflexi OTU9
Acidobacteria OTU166
Deltaproteob.-Desulfobulbaceae OTU538
Betaproteobacteria-Gallionella OTU817
Alphaproteob.-Rhodospirillaceae OTU465
Nitrospirae OTU851
Bacteroidetes-Bacteroidales OTU379
Bacteroidetes-Bacteroidales OTU268
Bacteroidetes-Chitinophagaceae OTU686
Bacteroidetes-Chitinophagaceae OTU190
Chlorobi-Ignavibacteriaceae OTU126
Chlorobi OTU43
Chloroflexi-Anaerolineae OTU258
Chloroflexi-Anaerolineae OTU12
Elusimicrobia OTU29
Elusimicrobia OTU897
Elusimicrobia OTU1
Deltaproteobacteria-Geobacter OTU825
Deltaproteobacteria-Syntrophaceae OTU39
Deltaproteobacteria OTU427
Betaproteobacteria-Neisseriaceae OTU129
Betaproteobacteria-Comamonadaceae OTU118
Bacteroidetes OTU515
Bacteroidetes OTU570
Chlorobi OTU218
Chloroflexi-Dehalococcoidaceae OTU216
Chloroflexi OTU259
Chloroflexi-Anaerolineae OTU332
Gemmatimonadetes OTU381
GOUTA4 OTU248
NC10 OTU313
AC1 OTU242
Actinobacteria OTU409
Deltaproteobacteria OTU269
Deltaproteobacteria-Geobacter OTU664
Deltaproteobacteria-Geobacter OTU154
Deltaproteobacteria-Geobacter OTU61
WS3 OTU41
Bacteroidetes OTU369
Chloroflexi-Anaerolineae OTU67
Chloroflexi-Anaerolineae OTU725
Deltaproteobacteria-Geobacter OTU618
Deltaproteobacteria-Geobacter OTU600
Deltaproteobacteria-Geobacter OTU555
Deltaproteobacteria-Geobacter OTU521
Deltaproteobacteria-Geobacter OTU58
Deltaproteobacteria-Geobacter OTU33
Deltaproteobacteria OTU362
Betaproteobacteria-Oxalobacteraceae OTU274
Bacteroidetes OTU834
Chloroflexi-Dehalococcoidetes OTU990
Chloroflexi-Anaerolineae OTU973
Chloroflexi-Anaerolineae OTU641
Armatimonadetes OTU688
non-incub.
CH4
CH4+ Fe3+
CH4+ Mn4+

Supplementary information that is intended for eventual online publication as Supporting Information is included in three MS-WORD files:

1. Rissanen_et_al_Supplemental_methods_1-3
    - contains detailed description of molecular methods (Supplemental Methods 1-3)
2. Rissanen_et_al_Supplementary_Figures_S1-S8
    - contains eight Supplementary figures, Figs. S1-S8
3. Rissanen_et_al_Supplementary_Table_S1
    - contains one Supplementary table, Table S1

Supplemental Methods 1 - 3

Supplemental Methods 1:

PCR, RT-PCR, preparation of the sequence libraries and sequencing

For each PCR amplicon library, two PCR reactions were performed. In the first round, PCR of the 16S rRNA gene amplicons was performed using the domain-specific primer pairs Arch340F (5'-CCCTAYGGGGYGCASCAG-3')/Arch1000R (5'-GGCCATGCACYWCYTCTC-3') (Gantner *et al*. 2011) for archaea and 27F (5'-AGAGTTTGATCMTGGCTCAG)/338R (5'-TGCTGCCTCCCGTAGGAGT-3') for bacteria. PCR of the *mcrA* gene amplicons was performed using the primer pair *mcrA* forward (5'-GGTGGTGTMGGATTCACACAR-3')/*mcrA* reverse (5'-TCATTGCRTAGTTWGGRTAGTT-3') (Beal, House and Orphan 2009). The M13 sequence (5'-TGTAAAACGACGGCCAGT-3') linker was attached to the 5' end of both Arch340F and the *mcrA* forward primers (Mäki, Rissanen and Tiirola 2016). In the first reaction for each gene, ~6 ng (2012), ~12 ng [2014, 0–10 cm layer of the profundal site ($P_{0\text{-}10}$)], or ~3 ng [2014, 10–30 cm layer of the profundal site ($P_{10\text{-}30}$)] of DNA was used as a template in a 25µl mixture containing 0.25 mM of dNTPs, 0.25 µM of both primers, 1 x Phusion Buffer, and 0.03 U/µl Phusion High-Fidelity DNA Polymerase. PCR amplification was performed in a C1000™ Thermal Cycler (Bio-Rad), with an initial denaturation step at 98ºC for 30 sec and 30 cycles of amplification (98ºC for 10 sec, 53ºC for 30 sec, and 72ºC for 60 sec) for the bacterial 16S rRNA gene amplicons and 35 cycles of amplification (98ºC for 10 sec, 55ºC for 30 sec, and 72ºC for 60 sec) for the archaeal 16S rRNA gene amplicons. There was an initial denaturation step at 98ºC for 60 sec and 29 cycles of amplification (98ºC for 60 sec, 50ºC for 60 sec, and 72ºC for 60 sec) for the *mcrA* gene amplicons. In the second PCR, 1 µl of first

round PCR products was used as a template in a 20 µl PCR mixture. The PCR conditions were similar to those described above, except that only six amplification cycles were run, an M13 primer was used as a forward primer in the amplification of the archaeal 16S rRNA and *mcrA* gene amplicons (Mäki, Rissanen and Tiirola 2016), and all the primers except for the Arch1000R included sequencing adaptors at the 5' end (A adaptor linked with forward primers 27F and M13; P1 adaptor linked with reverse primers 338R and *mcrA* reverse), as well as nucleotide barcodes incorporated between the A adapter and the forward primers to distinguish samples in the mixed reaction. PCR products were purified with Agencourt AMPure XP (Beckman Coulter), DNA concentration was measured using a Qubit 2.0 Fluorometer and a dsDNA HS Assay Kit (Thermo Fisher), and the samples were pooled in equal DNA amounts for each gene. The amplicon pool was further purified using AMPure XP.

The active methanogenic and methanotrophic archaeal population in $P_{0\text{-}10}$ in 2014 was studied using the reverse transcriptase PCR (RT-PCR) of *mcrA*. DNAse treatment to remove the DNA, followed by an RT reaction with random hexamers to transcribe the RNA (10–14 ng per 10 µl reaction) into cDNA, was performed using a Maxima H Minus First Strand cDNA Synthesis Kit with dsDNase (Thermo Fisher Scientific) according to the manufacturer's instructions. The PCR conditions for the cDNA were similar to those described above for the *mcrA* gene except that a lower concentration of polymerase was used (0.02 U/µl). In addition, 2 µl of RT product or RT controls (1. RTneg: DNAse + RT procedure without RT enzyme; 2. DNAse: DNAse treated sample without RT reaction) was utilized as a template in the first PCR reaction, from which 2 µl was utilized in the second PCR in a 21 µl total volume.

In order to adjust the length of the archaeal 16S rRNA gene amplicon (~660 bp) for the Ion Torrent™ sequencing (recommended ~400 bp), the fragments were cut shorter (Mäki,

Rissanen and Tiirola 2016). No fragmentation was performed for the bacterial 16S rRNA gene (< 400 bp) or *mcrA* gene amplicons (~500 bp). Although this might have slightly reduced the length and quality of the *mcrA* sequence reads (Mäki, Rissanen and Tiirola 2016), there were enough high-quality sequences left for the final analyses after post-sequencing quality control was performed (see below). Size selection, emulsion PCR, sequencing [Ion Torrent™ Personal Genome Machine (PGM)], and sequence filtering using PGM software were performed as described in the study by Mäki, Rissanen and Tiirola (2016).

Supplemental Methods 2:

Preparation of the *mcrA* gene database

The custom-made *mcrA* gene database was compiled of our initial in-house database and the database published by Yang *et al*. (2014). The sequences for our initial in-house database were retrieved from the EMBLALL database (via the SRS server LION, http://www.dkfz.de/srs) using the search query "description = mcrA BUTNOT un," which excluded hits from uncultured and unidentified microbes. The taxonomies of these sequences were then retrieved from the databases using an in-house script in EMBOSS (European Molecular Biology Open Software Suite). Furthermore, *mcrA* sequences of the ANME archaea, *Methanomassiliicoccales*, *Verstraetearchaeota*, and Miscellaneous Crenarchaeota group (*MCG*) (also referred to as *Bathyarchaeota*), as well as environmental sequences classified in those groups in the phylogenetic trees of previous papers (Ettwig *et al*. 2008; Lloyd, Alperin and Teske 2011; Yanagawa *et al*. 2011; Biddle *et al*. 2012; Borrel *et al*. 2013; Haroon *et al*. 2013; Evans *et al*. 2015; Vanwonterghem *et al*. 2016), were manually collected from the databases. This initial in-house database was then combined with that of Yang *et al*.

(2014), which included the *mcrA* sequences of only cultured methanogens and environmental sequences without taxonomies. Any duplicate sequences and sequences without taxonomies were removed from the combined database.

Supplemental Methods 3:

Validation and fine-tuning of the *mcrA* classification by phylogenetic tree analysis

A phylogenetic tree analysis (neighbor-joining method) of the amino acid sequences deduced from the *mcrA* gene using the representative sequences of the OTUs (in $P_{0\text{-}10}$ and $P_{10\text{-}30}$ in 2014) and a subset of the database sequences was performed with MEGA 6 (Tamura *et al*. 2013) to further validate and fine-tune the *mcrA*-classification (see Fig. S2, Supporting Information). This analysis assigned two OTUs and one OTU with only a kingdom-level classification (*Archaea*) into order *Methanomassiliicoccales* and phyla *Verstraetearchaeota*, respectively, two OTUs with only an order-level classification (*Methanosarcinales*) into ANME-2D, and four OTUs with only an order-level classification (*Methanomicrobiales*) into the *Methanoregulaceae* family.

References:

Beal EJ, House CH, Orphan VJ. Manganese- and iron-dependent marine methane oxidation. *Science* 2009;**325**:184-187.

Biddle JF, Cardman Z, Mendlovitz H *et al*. Anaerobic oxidation of methane at different temperature regimes in Guaymas Basin hydrothermal sediments. *ISME J* 2012;**6**:1018-1031.

Borrel G, O´Toole PW, Harris HMB *et al*. Phylogenomic data support a seventh order of methylotrophic methanogens and provide insights into the evolution of methanogenesis. *Genom Biol Evol* 2013;**5**:1769-1780.

Ettwig KF, Shima S, van de Pas-Schoonen KT *et al*. Denitrifying bacteria anaerobically oxidize methane in the absence of *Archaea*. *Environ Microbiol* 2008;**10**:3164-3173.

Evans PN, Parks DH, Chadwick GL *et al.* Methane metabolism in the archaeal phylum *Bathyarchaeota* revealed by genome-centric metagenomics. *Science* 2015;**350**:434-438.

Gantner S, Andersson AF, Alonso-Sáez L *et al*. Novel primers for 16S rRNA based archaeal community analyses in environmental samples. *J Microbiol Meth* 2011;**84**:12-18.

Haroon MF, Hu S, Shi Y *et al*. Anaerobic oxidation of methane coupled to nitrate reduction in a novel archaeal lineage. *Nature* 2013;**500**:567-570.

Lloyd KG, Alperin MJ, Teske A. Environmental evidence for net methane production and oxidation in putative ANaerobic MEthanotrophic (ANME) archaea. *Environ Microbiol* 2011;**13**:2548-2564.

Mäki A, Rissanen AJ, Tiirola MA. Practical method for barcoding and size-trimming PCR templates for amplicon sequencing. *BioTechniques* 2016;**60**:88-90.

Tamura K, Stecher G, Peterson D *et al*. MEGA6: Molecular evolutionary genetics analysis version 6.0. *Mol Biol Evol* 2013;**30**:2725-2729.

Vanwonterghem I, Evans PN, Parks DH. *et al*. Methylotrophic methanogenesis discovered in the archaeal phylum Verstraetearchaeota. *Nat Microbiol* 2016;**1**:16170; doi:10.1038/nmicrobiol.2016.170.

Yanagawa K, Sunamura M, Lever MA *et al*. Niche separation of methanotrophic archaea (ANME-1 and -2) in methane-seep sediments of the Eastern Japan sea offshore Joetsu. *Geomicrobiol J* 2011;**28**:118-129.

Yang S, Liebner S, Alawi M *et al*. Taxonomic database and cut-off value for processing *mcrA* gene 454 pyrosequencing data by MOTHUR. *J Microbiol Methods* 2014;**103**:3-5.

Supporting information. Figures S1-S8

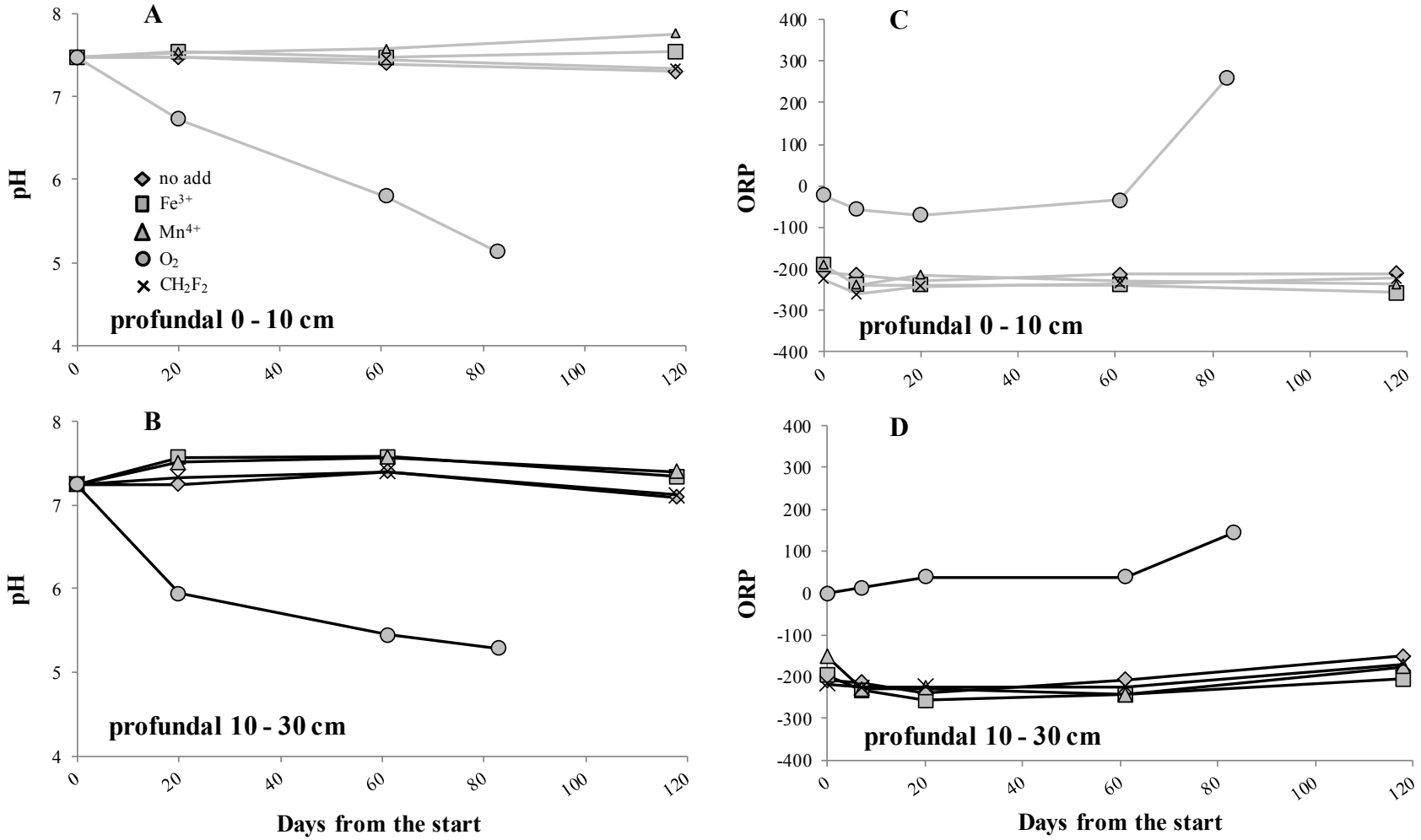

Figure S1. pH at four time points during the incubation of sediment slurries collected from the (A) 0–10 cm ($P_{0\text{-}10}$) and (B) 10– 30 cm ($P_{10\text{-}30}$) layers of profundal sediments in 2014 and amended without anything (no addition) or with Fe^{3+}, Mn^{4+}, O_2, or CH_2F_2. (C) and (D) are the same as (A) and (B), but for the oxidation reduction potential (ORP).

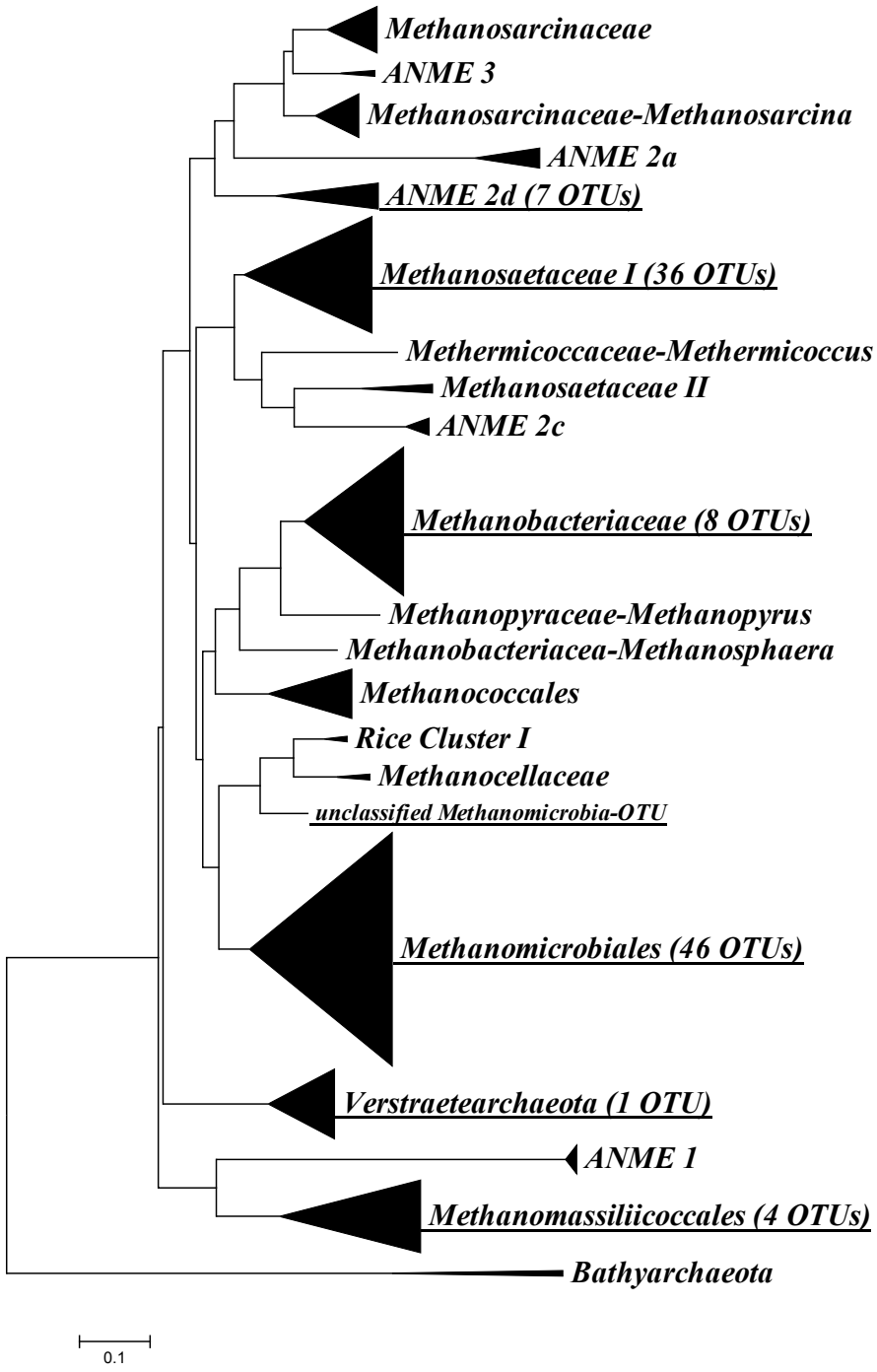

Figure S2. Phylogenetic tree (neighbor-joining method) of the amino acid sequences deduced from the methyl-coenzyme M reductase (*mcrA*) gene, which includes database sequences and the representative sequences of the operational taxonomical units (OTUs) (at a 96% similarity level) detected in 0 – 10 cm ($P_{0\text{-}10}$) and 10 – 30 cm ($P_{10\text{-}30}$) layers of the profundal site in 2014. The names of the phylogenetic clusters harboring the OTU sequences are underlined.

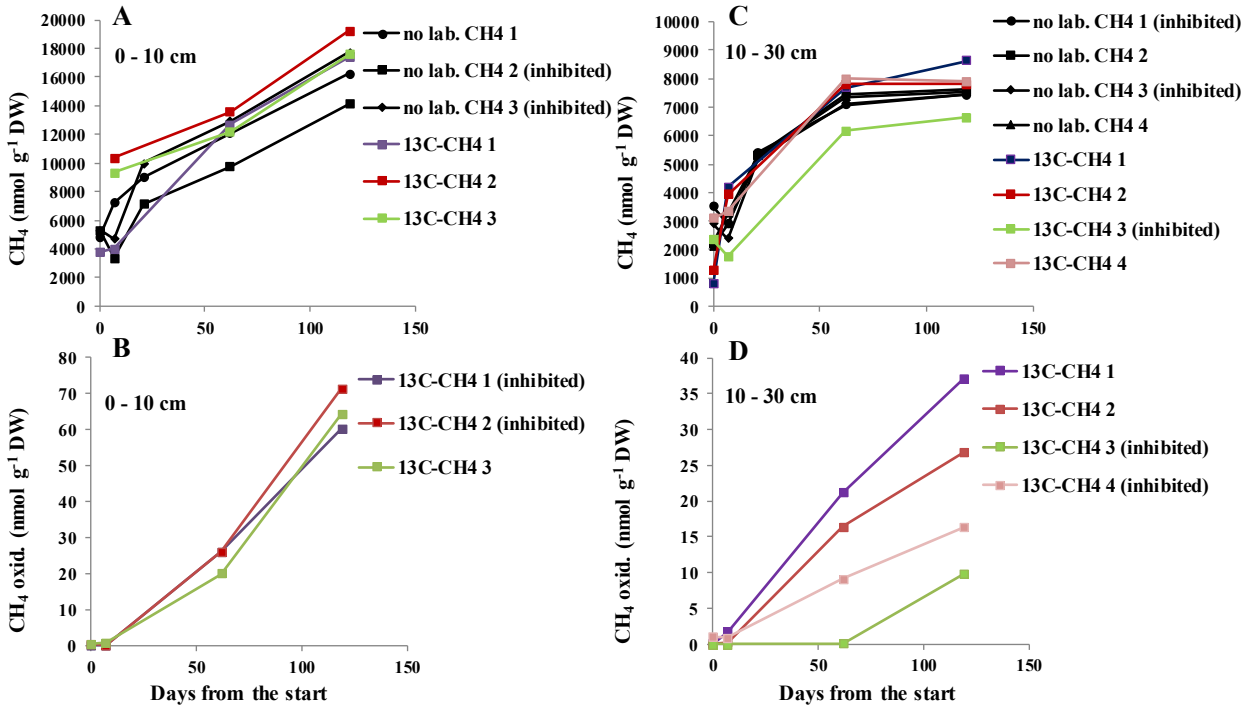

Figure S3. Cumulative (A) CH_4 production and (B) CH_4 oxidation (based on $^{13}CO_2$ production) in the incubation bottles of sediment slurries collected from the 0–10 cm layer ($P_{0\text{-}10}$) of the profundal site and amended with CH_4+CH_2F_2 (^{13}C-labelled CH_4 and CH_4 with no label). (C) and (D) are the same as (A) and (B), but for the 10–30 cm layer ($P_{10\text{-}30}$) of the profundal site. Bottles where the CH_4 production or oxidation was inhibited by CH_2F_2, that is, where it did not increase between the first two time points, are indicated in the symbol description. The CH_4 concentration measurements for bottles ^{13}C-CH_4 2 and ^{13}C-CH_4 3 of $P_{0\text{-}10}$ on day 1 failed (in A). However, based on the relatively high CH_4 concentration during the second time point, it is very likely that CH_4 production was not inhibited between the first two time points in these bottles.

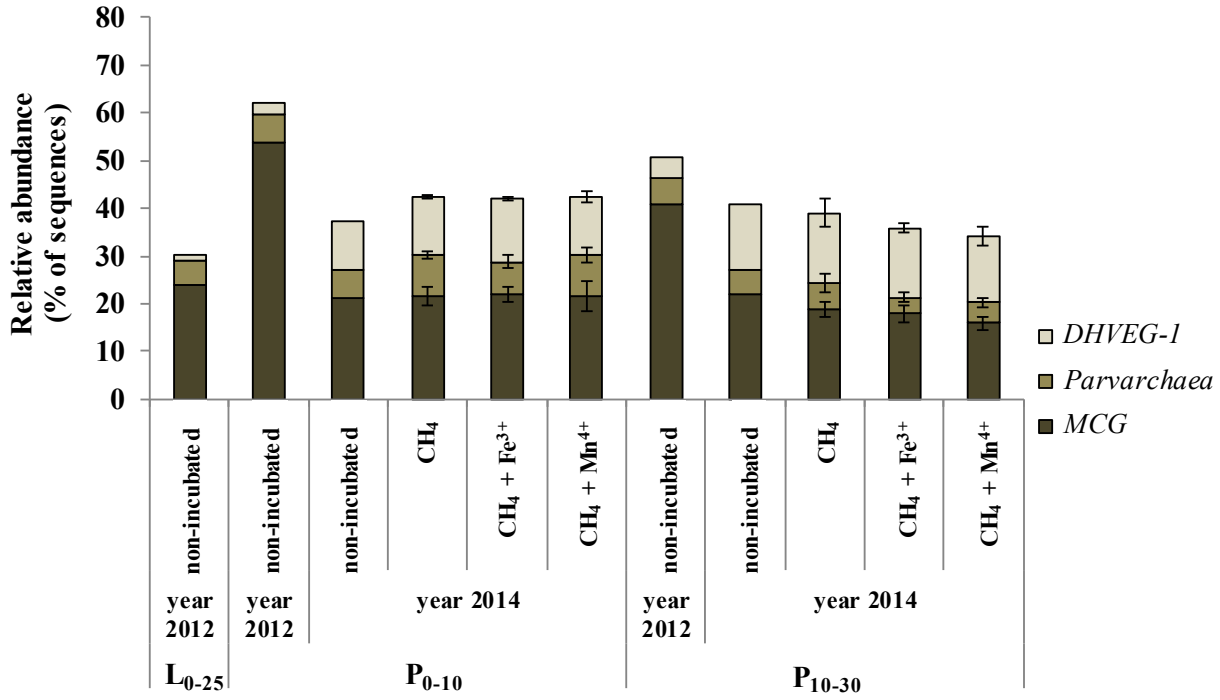

Figure S4. Relative abundances (average +/- SD) of the taxonomic groups of dominant non-methanogenic archaea in the study sediments based on 16S rRNA gene sequencing. $L_{0\text{-}25}$, $P_{0\text{-}10}$ and $P_{10\text{-}30}$ denote 0 – 25 cm layer of the littoral and 0 – 10 cm and 10 – 30 cm layers of the profundal study site, respectively.

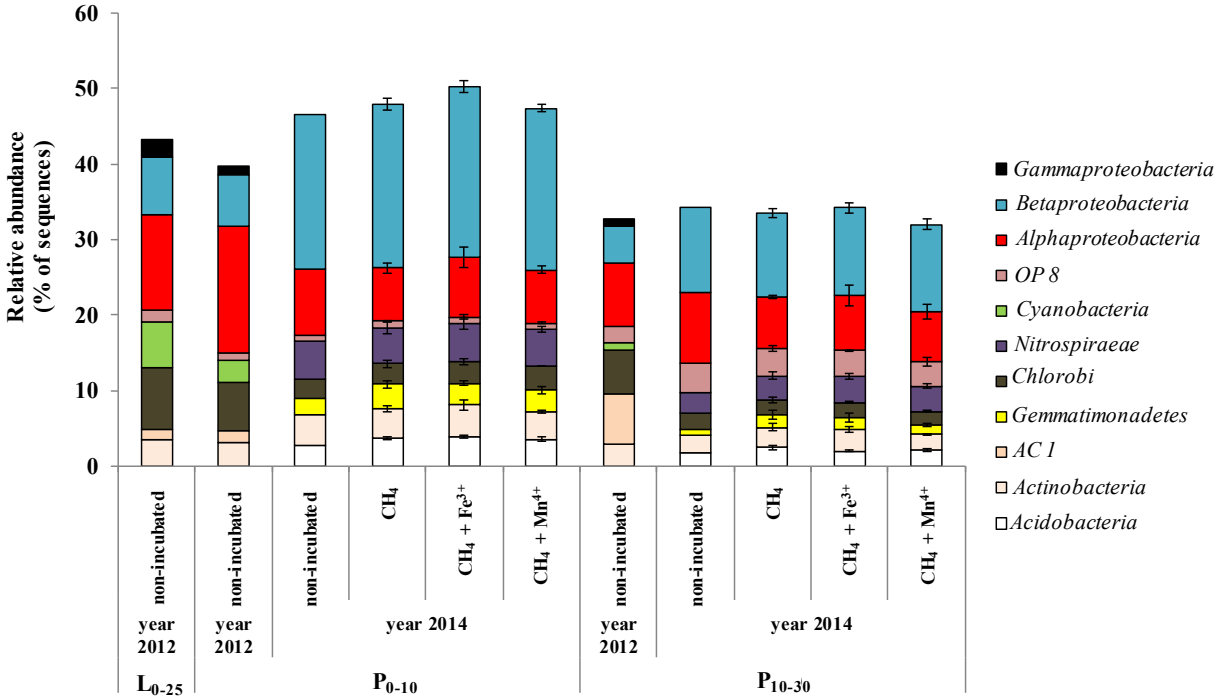

Figure S5. Relative abundances (average +/- SD) of the taxonomic groups of the other abundant bacteria. $L_{0\text{-}25}$, $P_{0\text{-}10}$ and $P_{10\text{-}30}$ denote 0 – 25 cm layer of the littoral and 0 – 10 cm and 10 – 30 cm layers of the profundal study site, respectively.

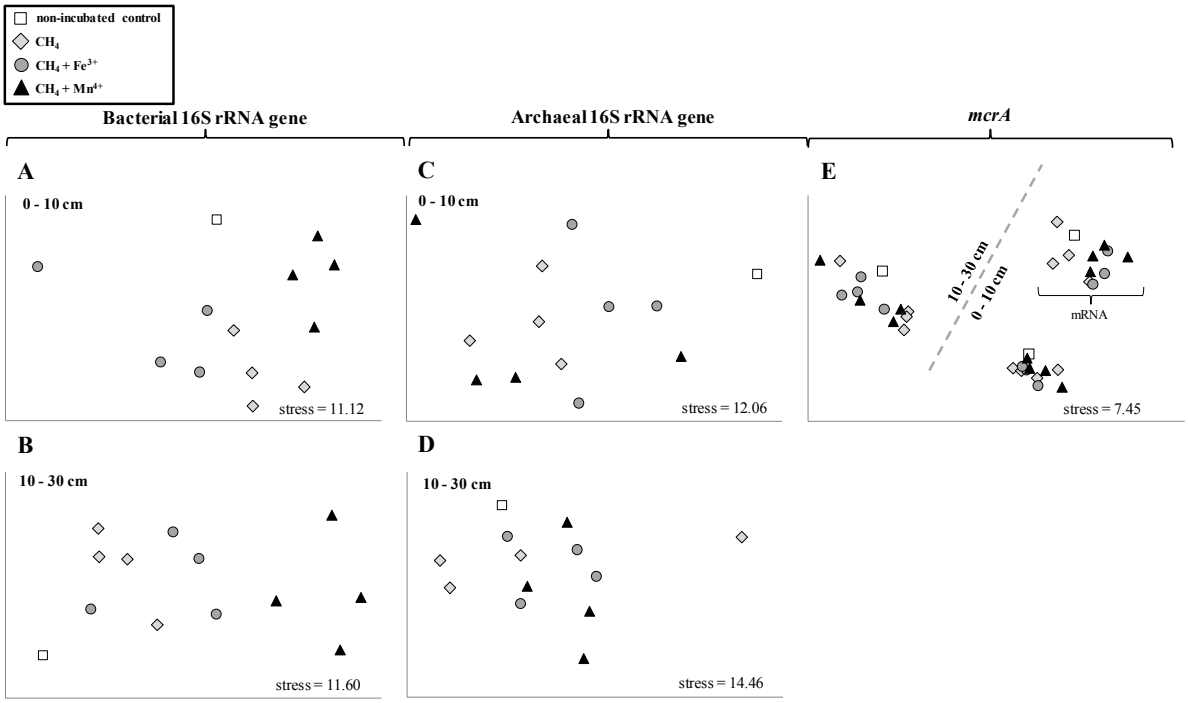

Figure S6. Non-metric multidimensional scaling analyses of the variation in the community structure of (A–B) bacteria (16S rRNA gene), (C–D) archaea (16S rRNA gene), and (E) methanogenic/methanotrophic archaea (*mcrA* gene), as well as the active methanogenic/methanotrophic archaea (mRNA transcripts of *mcrA*) before (non-incubated sample) and after the incubations of sediment slurries collected from the 0–10 cm ($P_{0\text{-}10}$) (A, C, E) and 10–30 cm ($P_{10\text{-}30}$) layers (B, D, E) of the profundal site in 2014 and amended with CH_4, CH_4+Fe^{3+}, or CH_4+Mn^{4+}. Due to the substantial differences between $P_{0\text{-}10}$ and $P_{10\text{-}30}$ in the primary NMS ordinations of the archaeal and bacterial 16S rRNA gene sequence data (data not shown), the final NMS ordination was performed separately for the two depth layers (A–D).

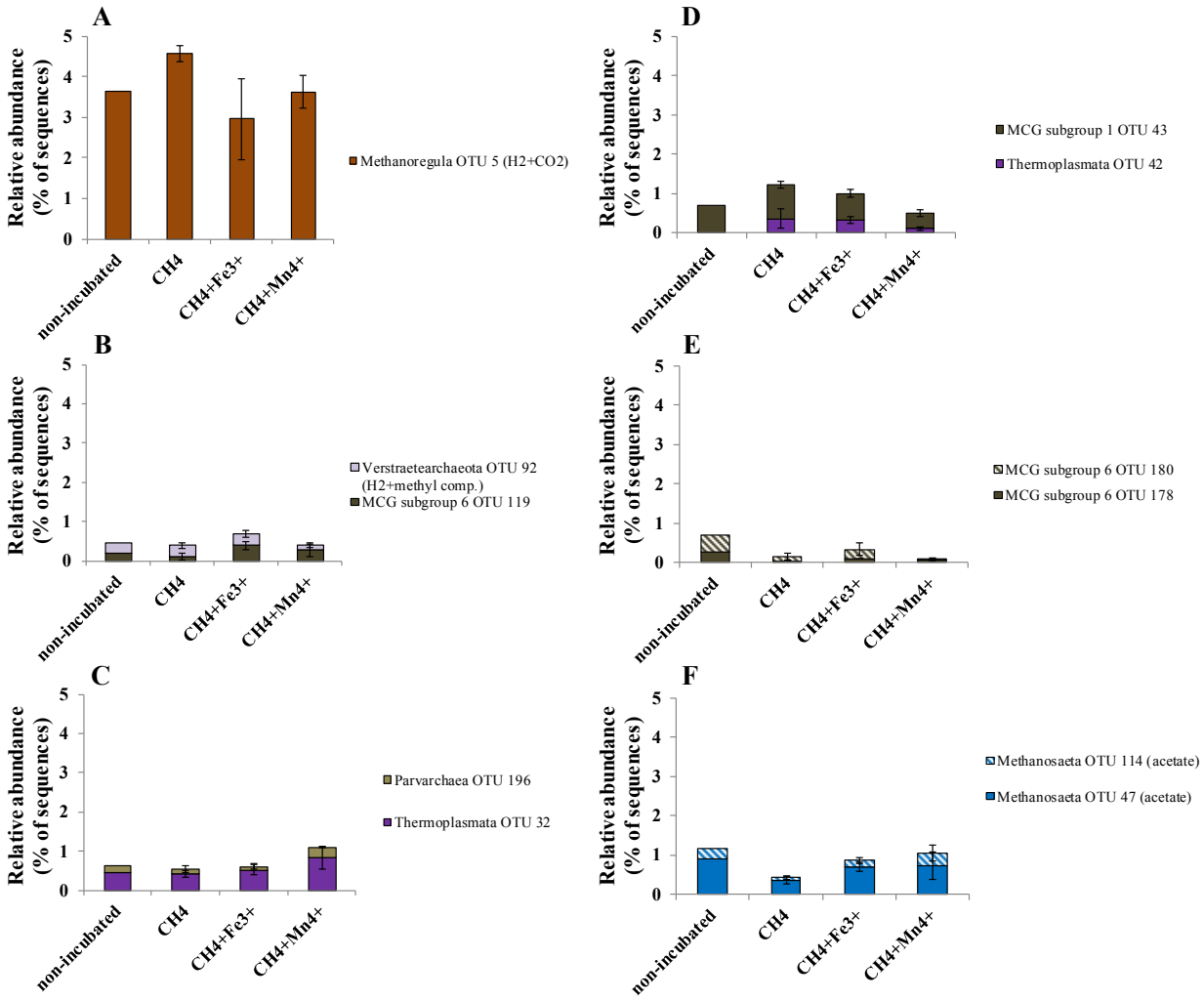

Figure S7. Relative abundance (average +/- SD) and taxonomic affiliations (and methanogenic substrate) of the archaeal 16S rRNA gene OTUs that differed in relative abundance among the CH_4, CH_4+Fe^{3+}, or CH_4+$Mn4^{+}$ treatments after the incubation of sediment slurry samples from the 0–10 cm ($P_{0\text{-}10}$) (A–C) and 10–30 cm ($P_{10\text{-}30}$) (D–F) layers (linear discriminant analysis [LDA] effect size [LEfSe] method $p < 0.05$). The OTUs are grouped into three rows according to the treatment in which they exhibited the highest relative abundance in comparison to the other treatments: (A)/(D) CH_4, (B)/(E) CH_4+Fe^{3+}, or (C)/(F) CH_4+Mn^{4+}.

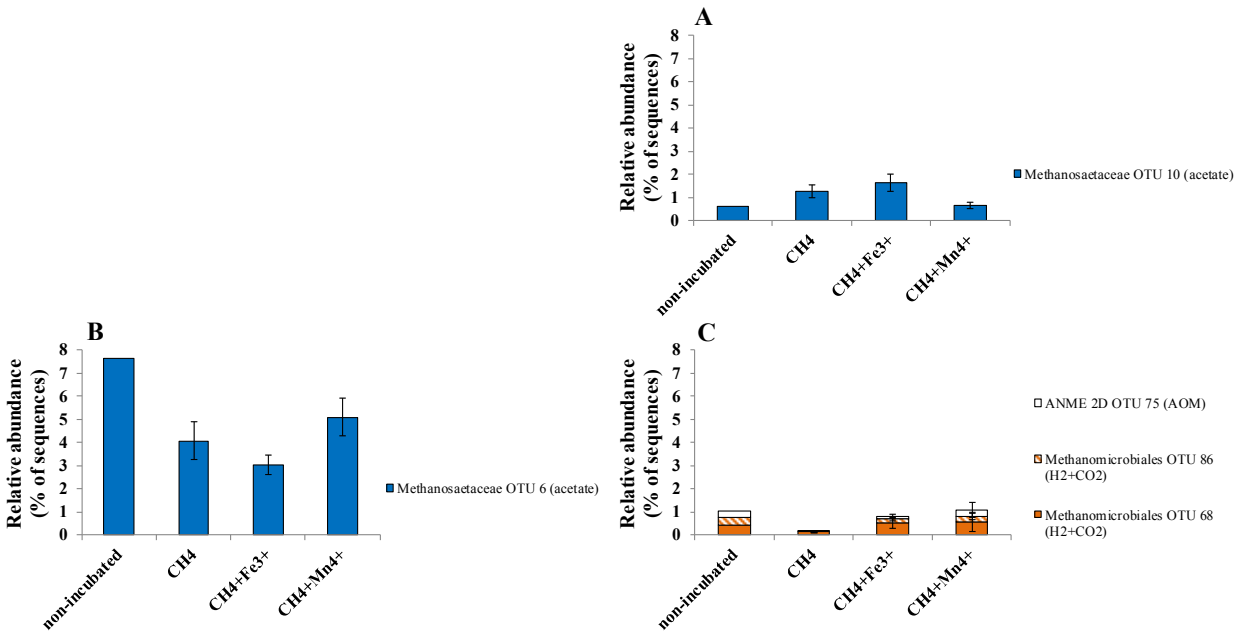

Figure S8. Relative abundance (average +/- SD) and taxonomic affiliations (and methanogenic substrate) of the *mcrA* gene OTUs that differed in their relative abundance among the CH_4, CH_4+Fe^{3+}, or CH_4+Mn^{4+} treatments after the incubation of sediment slurry samples from the 0–10 cm ($P_{0\text{-}10}$) (B) and 10–30 cm ($P_{10\text{-}30}$) (A, C) layers (linear discriminant analysis [LDA] effect size [LEfSe] method $p < 0.05$). The OTUs are grouped into two rows according to the treatment in which they exhibited the highest relative abundance in comparison to the other treatments: A) CH_4+Fe^{3+} or (B)/(C) CH_4+Mn^{4+}.

Supporting information. Table S1.

Table S1. Oxidation reduction potential (ORP) and pH at the end of the incubations of the sediment slurry samples subjected to different treatments in 2012 and 2014, as well as the pH at the start of the incubations in 2012. The values are shown as averages ± SD, n = 3–4. $L_{0\text{-}25}$, $P_{0\text{-}10}$, $P_{10\text{-}30}$, $P_{90\text{-}130}$, $P_{390\text{-}410}$ denote 0 – 25 cm layer of the littoral and 0 – 10 cm, 10 – 30 cm, 90 – 130 cm and 390 – 410 cm layers of the profundal study site, respectively.

Year	Sample code	Treatment	pH	ORP (mv)
2012[1]				
	$L_{0\text{-}25}$	start	6.55	
		CH_4	6.55±0.08	-185.8±33.3
		CH_4+SO_4^{2-}	6.49±0.02	-72.5±18.4
		CH_4+NO_3^-	6.46±0.05	-56.3±29.9
		CH_4+O_2	5.47±0.49	-79.0±43.7
	$P_{10\text{-}30}$	start	6.54	
		CH_4	6.55±0.11	-335.3±7.9
		CH_4+SO_4^{2-}	6.59±0.10	-215.3±21.1
		CH_4+NO_3^-	6.59±0.01	-222.3±24.4
		CH_4+O_2	5.22±0.13	-204.8±27.7
	$P_{90\text{-}130}$	start	6.38	
		CH_4	6.39±0.10	+21±17.4
		CH_4+SO_4^{2-}	6.38±0.08	-74.3±12.5
		CH_4+NO_3^-	6.23±0.16	-58.3±74.2
		CH_4+O_2	5.08±0.06	-128.0±25.7
	$P_{390\text{-}410}$	start	6.59	
		CH_4	6.60±0.07	-218.3±100.6
		CH_4+SO_4^{2-}	6.62±0.03	-232.0±44.3
		CH_4+NO_3^-	6.52±0.04	-335.0±7.2
		CH_4+O_2	5.69±0.16	-337.3±6.0
2014[1]				
	$P_{0\text{-}10}$	CH_4	7.27±0.05	-207.0±8.1
		CH_4+Fe^{3+}	7.54±0.04	-257.8±4.0
		CH_4+Mn^{4+}	7.75±0.01	-236.8±4.3
		CH_4+O_2	5.13±0.18	+259.3±75.8
		CH_4+CH_2F_2	7.33±0.01	-223.7±2.5
	$P_{10\text{-}30}$	CH_4	7.09±0.00	-146.0±9.7
		CH_4+Fe^{3+}	7.34±0.02	-205.5±3.7
		CH_4+Mn^{4+}	7.40±0.02	-176.5±11.5
		CH_4+O_2	5.29±0.11	+145±20.1
		CH_4+CH_2F_2	7.12±0.02	-170.8±1.7

1) Incubations were done at +4°C for up to 14 months in 2012 and at +10°C for up to 4 months in 2014